

Evaluation and Improvements of Cloud and Precipitation Physics in the Operational Hurricane WRF Model at NOAA/EMC

US Weather Research Program/Joint Hurricane Testbed
PI: Yuqing Wang and co-I: Vaughan Phillips (left July 2011)
University of Hawaii at Manoa, Honolulu, HI 96822

Yuqing Wang: phone: (808)956-5609, email: yuqing@hawaii.edu

Vaughan Phillips in UK now and no longer a co-I

Grant Number: NA09OAR4310081

Report Period: August 1, 2009-January 31, 2012

OVERALL GOAL

The overall goal of this project is to evaluate and improve the cloud and precipitation physics used in the operational Hurricane Weather Research and Forecast (HWRF) model developed in the Environmental Modeling Center (EMC) at the National Centers for Environmental Prediction (NCEP) of NOAA, achieving improved prediction of hurricane structure and intensity, including the size, by the HWRF model at NCEP/EMC.

SPECIFIC OBJECTIVES

We will first evaluate and identify possible discrepancies in the current cloud and precipitation physics used in the HWRF model and understand how these discrepancies may affect the hurricane structure and intensity. This will be done by implementing the current schemes into the hurricane model TCM4 developed by the PI and conduct sensitivity experiments that are designed with both real cases and idealized simulations. The focus is given to both grid-scale moist processes and subgrid scale convective processes in the HWRF model. Both are critical to the realistic representation of three-dimensional (3D) diabatic heating, which is believed to be the key to both the structure and intensity of hurricanes. We will then closely work with the members of the HWRF model development team at NCEP/EMC to improve the relevant aspects of the cloud and precipitation scheme used in the HWRF model at NCEP/EMC. The following four specific objectives will be achieved:

- To diagnose the discrepancies of the current cloud and precipitation physics and the interaction between grid-scale moist processes and subgrid-scale convection in the HWRF model and to understand how they affect hurricane intensity and structure, including size;
- To improve the representation of the cloud and precipitation physics in the HWRF model based on the PI and co-I's previously results and evaluate the performance of the modified schemes through model inter-comparison between the HWRF model and TCM4;
- To test and tune the modified schemes in the experimental prediction mode and to evaluate their overall improvements in predicting hurricane structure and intensity using the HWRF model hindcasts for the cases in the 2010 hurricane season;
- To document the modified schemes with both technical and scientific details and to provide training to the members of the HWRF model development team at NCEP/EMC.

APPROACH

The approach to achieve our goal is to conduct numerical experiments using the HWRf model, the hurricane model–TCM4, and the single-column parcel model–SCPM with bulk and spectral microphysics schemes. The SCPM will be used to create a multi-dimensional lookup table for the supersaturation as a function of vertical velocity and other model parameters, refining the bulk scheme to be used operationally, and will be embedded in the convection scheme. The TCM4 will be used to diagnose the discrepancies of the current schemes used in the HWRf model in simulating hurricane intensity and size changes. We will implement the current cloud and precipitation schemes used in the HWRf model into TCM4 and perform a suite of idealized numerical experiments to help isolate the effects of individual processes and understand their combined impacts. In this regard, TCM4 can be regarded as a diagnostic tool to help identify the key physical processes. Based on the inter-model evaluation, we will modify the current relevant modules in the HWRf model or replace them with more advanced/improved schemes to better represent the cloud and precipitation physics in the HWRf model and to achieve improved prediction of hurricane intensity and structure at NCEP/EMC.

WORKS COMPLETED

We completed the following tasks during the period 08/01/2009-07/31/2011:

- (1) To have diagnosed the discrepancies of the current cloud microphysics physics;*
- (2) To have examined the interaction between grid-scale moist processes and subgrid-scale convection in the HWRf model to understand how they affect hurricane intensity and structure, including size;*
- (3) To have analyzed the potential discrepancies of the current dynamical core of the HWRf model and the improvements of precipitation physics in HWRf;*
- (4) To have developed and tested the single column parcel model (SCPM).*
- (5) To have examined the potential effect of the initial vortex size on the subsequent size change in the model prediction;*
- (6) To have revealed the importance of the initial radial tangential wind profile to the size change in hurricane models;*
- (7) To have developed a resolution-independence warm rain cloud microphysics scheme based on satellite observations, which may be applied for high-resolution atmospheric models, such as in the HWRf model outer domains.*

We have completed the following tasks during this reporting period (08/01/2011-01/31/2012):

- (1) To have set up a real-time forecast system for the western Pacific locally in the University of Hawaii using the WRF model*
- (2) To have developed a new dynamical initialization scheme for tropical cyclone models and evaluated its application in the real-time forecasting system for 2010 and 2011.*
- (3) To have installed the EMC HWRf for North Atlantic and performed a case study to diagnose/evaluate the new physics parameterization schemes in the HWRf model.*

First project year (08/01/2009-07/31/2010)

As the first step, we have implemented the current cloud microphysics scheme and convective parameterization scheme used in the HWRf model into TCM4 and conducted sensitivity experiments to identify those aspects that considerably affect the spatial distribution of diabatic heating and thus on the model hurricane structure and intensity, including the storm

size. The 3D distribution of diabatic heating from both subgrid cumulus convection and grid-scale moist processes are the key to the hurricane structure and intensity. We have compared the structure, intensity, and diabatic heating of the HWRF model cloud microphysics scheme with that used in TCM4. We have examined the possible effect of cumulus convective parameterization scheme in coarse model domains on the fine-resolution explicit simulations of hurricanes in TCM4. These comparisons have helped us identify the potential discrepancies of the current cloud and precipitation physics used in the HWRF model and elucidate the physical mechanisms and also provide the basis for our improvements of the HWRF cloud and precipitation physics in the coming project year.

We have also extended our diagnostics of cloud and precipitation physics to examine the possible discrepancies in the dynamical core of the HWRF model in comparison with the simulation using the WRF_ARW dynamical core with the same model physics options. It is our purpose to see whether biases in the prediction of hurricane size and intensity by HWRF are related to the dynamical core. Hurricane Katrina (2005) was selected in this comparison. Our results show that in terms of storm intensity prediction by HWRF, two aspects need to be addressed: why the initial surface wind speed and the intensity of the storm are weak and why the simulated maximum surface wind intensified much slower than the central surface pressure deepened. Although the NMM dynamical core simulated weaker hurricane intensity, it simulated the track considerably better in terms of the landfall timing and location than the ARW dynamical core for the Hurricane Katrina case. This indicates that the NMM dynamical core might capture the evolution of the large-scale environmental flow, which is the key to the accurate prediction of storm motion. However, the storm intensity is largely controlled by the inner core dynamics, which was not well represented by the numerical scheme in the NMM dynamical core and needs to be improved. The difference in the vertical structure of the simulated storm suggests that some discrepancies between the simulations with different dynamical core might be related to the difference in the vertical discretization. We also found that the dynamical core may affect the cloud microphysics to some degree. This has never been recognized. Therefore, a systematic diagnostics of the dynamical core of the NMM is required in order to improve the prediction of storm intensity and structure by HWRF.

In accordance with the work-plan of the project, during Year 1 we have also developed and tested a single-column parcel model (SCPM). The SCPM represents how the supersaturation is maintained close to water saturation by an approximate balance between the adiabatic cooling from ascent and condensation, in this mixed-phase region, while the liquid fraction is close to unity. This SCPM will have two roles for improving forecasts with the HWRF model in the second project year: (1) to provide improved parameterization of supersaturation and other microphysical quantities (e.g. liquid fraction) assumed to treat the grid-resolved clouds; (2) to embed the SCPM inside the deep convection parameterization, providing better estimates of convective heating aloft and detrainment of condensate mass.

Second project year (08/01/2010-07/31/2011)

We have tried to understand what factors and physical processes that control the size change in hurricane models. This is the key to the evaluation of model cloud and precipitation physics. Without this knowledge, it is hard to place our efforts to improve the model physics. According the efforts we made in the first project year, we suspect that the initial vortex structure is the potential candidate that results in the subsequent rapid size increase in the current HWRF model. Therefore, we have done a systematic evaluation on this issue based both HWRF and TCM4. We first examined how the initial size (here we refer to size as the initial radius of maximum wind-RMW) of the model storm may affect the subsequent size change in the models. We found that the big storm (with large initial RMW) grew continuously during the model integration while the small storm (with small initial RMW) could maintain its small size. This indicates that the initial vortex in the HWRF might be too big at the initial time. In addition, the model resolution at 9 km might be a reason too since at this resolution the model could not resolve the observed RMW. As a result, higher resolution may be needed in order to improve the size prediction by the HWRF model.

Similar to the initial size of the model vortex, we found a crucial impact of the radial wind profile at the initial time on the predicted evolution of hurricane size in the models. It is found that even though the storms have the same initial RMW, those with broad radial wind profile would grow much faster than the narrow vortices that have a rapid decaying profile of tangential wind with radius at the initial time. This is mainly due to the existence of vorticity skirt for the slow decaying wind profiles, which have large inertial stability outside the eyewall, preventing the contraction of the RMW at the early stage of model integration. At later stage, the broad profile favors large surface flux and formation of outside rainbands and diabatic heating outside the eyewall. This leads to a considerable increase in storm size in the prediction. We examined the initial structure of hurricanes in HWRF and found that this is the most likely the candidate for the size increase in the current HWRF, indicating a need to improve the representation of the initial vortex structure in the operational HWRF model.

Since the new version 3.2 of the HWRF model will be released in April 2011, we have already worked on the new physics in the next version HWRF model. We have implemented the new GFS cumulus parameterization scheme into TCM4 and started to perform some initial test runs with both TCM4 and HWRF model. The PI is a member of the WRF model development team and also implemented a modified Tiedtke cumulus parameterization scheme into the whole WRF model system. This provides an opportunity to intercompare different cumulus parameterization schemes in the HWRF model version 3.2. We indeed have helped identify some bugs in the WRF system that will be released in April 2011.

Non-cost extension period (08/01/2011-01/31/2012)

To achieve our goal and have close monitoring on the model performance, we have implemented the HWRF model in a real-time forecast mode early this year. This will be a testbed for our planned improvements to the model physics in the rest of the project year. This is a milestone for this project and for follow-up possible JHT projects.

HIGHLIGHTS OF RESULTS

To diagnose the discrepancies of the current cloud microphysics and the interaction between grid-scale moist processed and subgrid-scale convection in the HWRF model and to understand how they affect hurricane intensity and structure, we have implemented both HWRF cloud microphysics scheme and the simplified Arakawa-Schubert (SAS) cumulus convective parameterization scheme into the hurricane model TCM4 and conducted a series of numerical experiments. We have also examined the potential discrepancies in the dynamical core and the potential sensitivity of the predicted hurricane size to the initial size and structure of the model storms. We have already set up a real-time forecast system for the eastern Pacific hurricanes using the HWRF model. Here we will highlight some of our results and their implications for the rest of our project year. To have a tracking record, we kept the highlights reported in the first project year below. The highlights for the results obtained during this reporting period are given in the second half of this section.

First project year (08/01/2009-07/31/2010)

a. Comparison of the Ferrier scheme in HWRF with the TCM4 mixed-phase scheme

Currently TCM4 uses a bulk mixed-phase cloud microphysics scheme. It predicts mixing ratios of water vapor, cloud water, rainwater, cloud ice, snow and graupel, with thirty six microphysics processes. The HWRF model uses the Ferrier microphysics scheme, which considers four hydrometeors, namely, suspended cloud liquid droplets, rain, large ice, and small ice. It only calculates the horizontal and vertical advectations of the total condensate, namely, the sum of all four hydrometeors and thus the scheme is relatively more economical in computation. The components of hydrometeors are then diagnosed based on some semi-empirical formulations. We have performed two idealized simulations using the two schemes in TCM4. The experimental design follows Wang (2007) except for 32 vertical levels and relatively larger nested meshes and finer finest mesh resolution (2 km) are used in this project. This aims at to see whether the HWRF cloud microphysics may result in any unexpected systematic difference from more sophisticated bulk cloud microphysics scheme, such as the mixed phase cloud microphysics scheme used in TCM4.

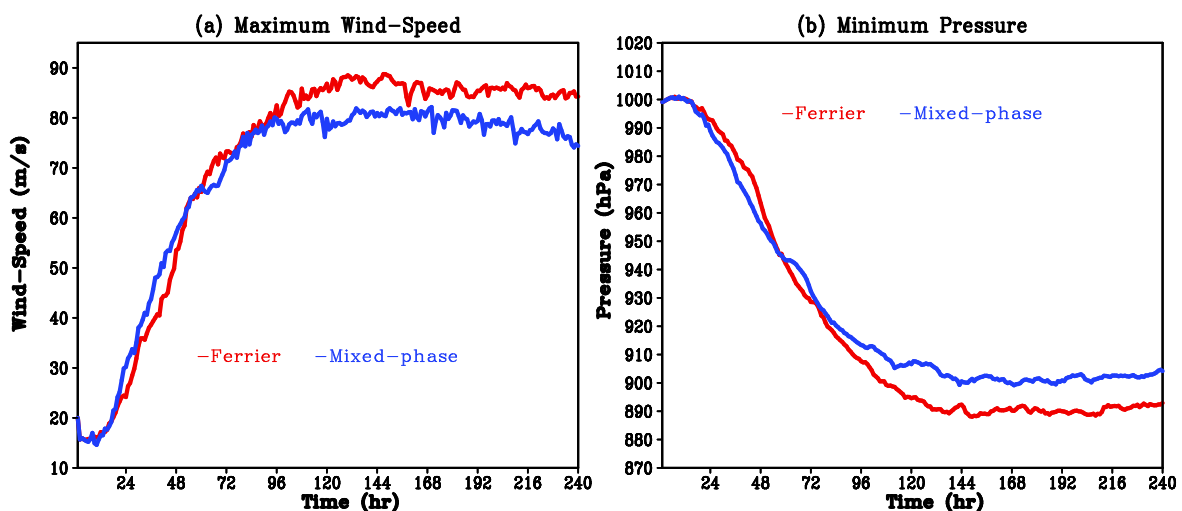


Figure 1. (a) The maximum azimuthal mean wind speed at the lowest model level (about 35 m above sea level); (b) the minimum sea level pressure of the simulated storms using Ferrier (red) and Wang (blue) cloud microphysics schemes in TCM4.

Figure 1 shows the time evolution of the maximum azimuthal mean wind speed at the lowest model level and the minimum sea level pressure of the simulated storm in TCM4 using the HWRF and TCM4 cloud microphysics schemes. It is interesting to see that the initial spin-up of the model storm using the Ferrier cloud microphysics scheme is slower than the TCM4 mixed phase scheme in the first 48 h of simulation. However, the subsequent intensification rate is large with the Ferrier scheme, which eventually produces a stronger storm than that with the TCM4 cloud microphysics scheme. Further the storm simulated with the Ferrier scheme does not show any increase in the radius of maximum azimuthal mean wind. This is in contrast with that simulated with the TCM4 cloud microphysics scheme (Fig. 2).

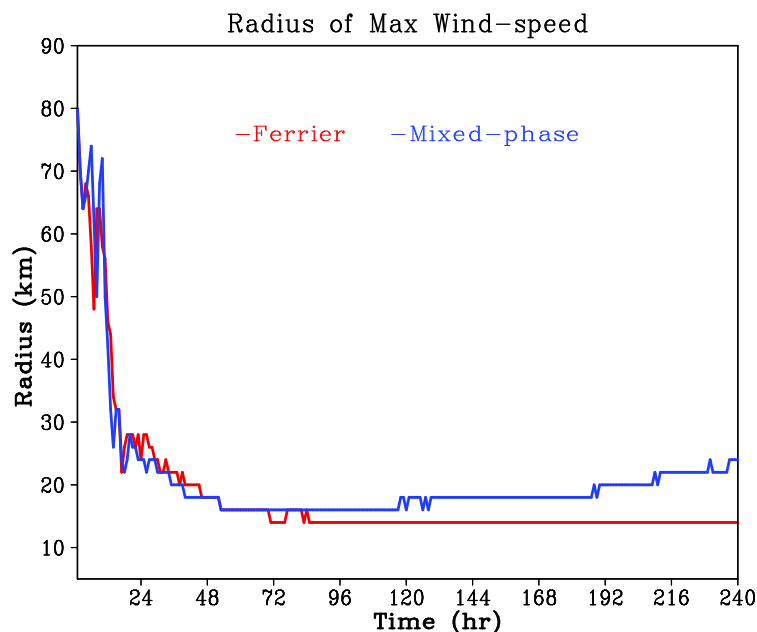


Figure 2. Time evolution of the radius of maximum azimuthal mean wind speed of the simulated storms in TCM4 with different microphysics scheme (red: Ferrier scheme, blue: TCM4 mix-phase scheme).

The results thus suggest that too big hurricanes predicted by HWRF model are unlikely due to the cloud microphysics scheme used. Consistent with the findings by Wang (2009), the larger storm with the TCM4 cloud microphysics corresponds to the rainfall (Fig. 3) and diabatic heating rate (Fig. 4) extending to larger radii. Further the azimuthally averaged diabatic heating rate by the TCM4 scheme tilt radially outward more than the Ferrier scheme because the latter simulated smaller radius of maximum wind (Fig. 2). Detailed examinations show that the simulated ice hydrometeors using the two schemes are quite different. For example, the Ferrier scheme produces much less stratiform clouds as well as much less anvil clouds outside the eyewall than the mixed phase scheme used in TCM4 (Fig. 5). This is also consistent with much smaller heating rate outside the eyewall and smaller radius of maximum azimuthal mean wind due to the lack of strong spiral rainbands (Figs. 3 and 4).

In summary, the Ferrier cloud microphysics scheme performs reasonably well in TCM4. Results show that the initial spin up of the model storm is slower using the Ferrier scheme than

the Wang scheme used in TCM4. However, the subsequent storm is stronger in the former than in the latter. The Ferrier scheme produces much less stratiform clouds and anvil clouds outside the eyewall due to the lack of strong spiral rainbands. As a result, the diabatic heating and ice hydrometeors are concentrated mainly in the eyewall region. This is also responsible for the simulated smaller radius of maximum azimuthal mean wind. These results suggest that the slow intensification and fast growth of the storm size in the operational HWRF model may not result from the discrepancies in the cloud microphysics scheme used. However, caution needs to be taken for this statement. The results we show are based on 2 km mesh simulation. It is not clear the difference would become smaller or larger if the horizontal resolution similar to that used in the operational HWRF is used. We plan to do sensitivity experiments to learn about the resolution dependency.

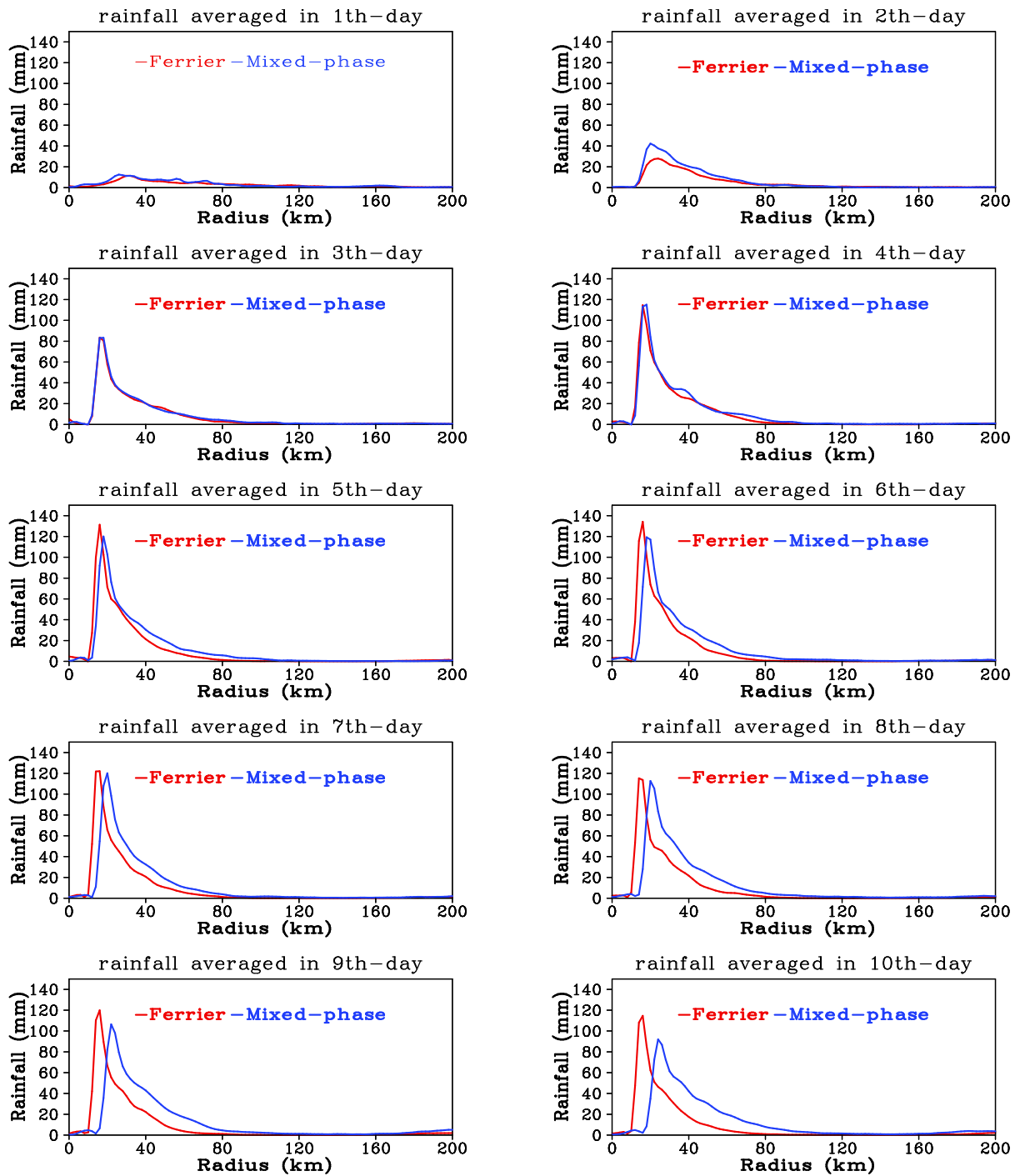


Figure 3. The azimuthal mean rainfall averaged in each 24h of simulation (red: Ferrier, blue: TCM4 mixed-phase).

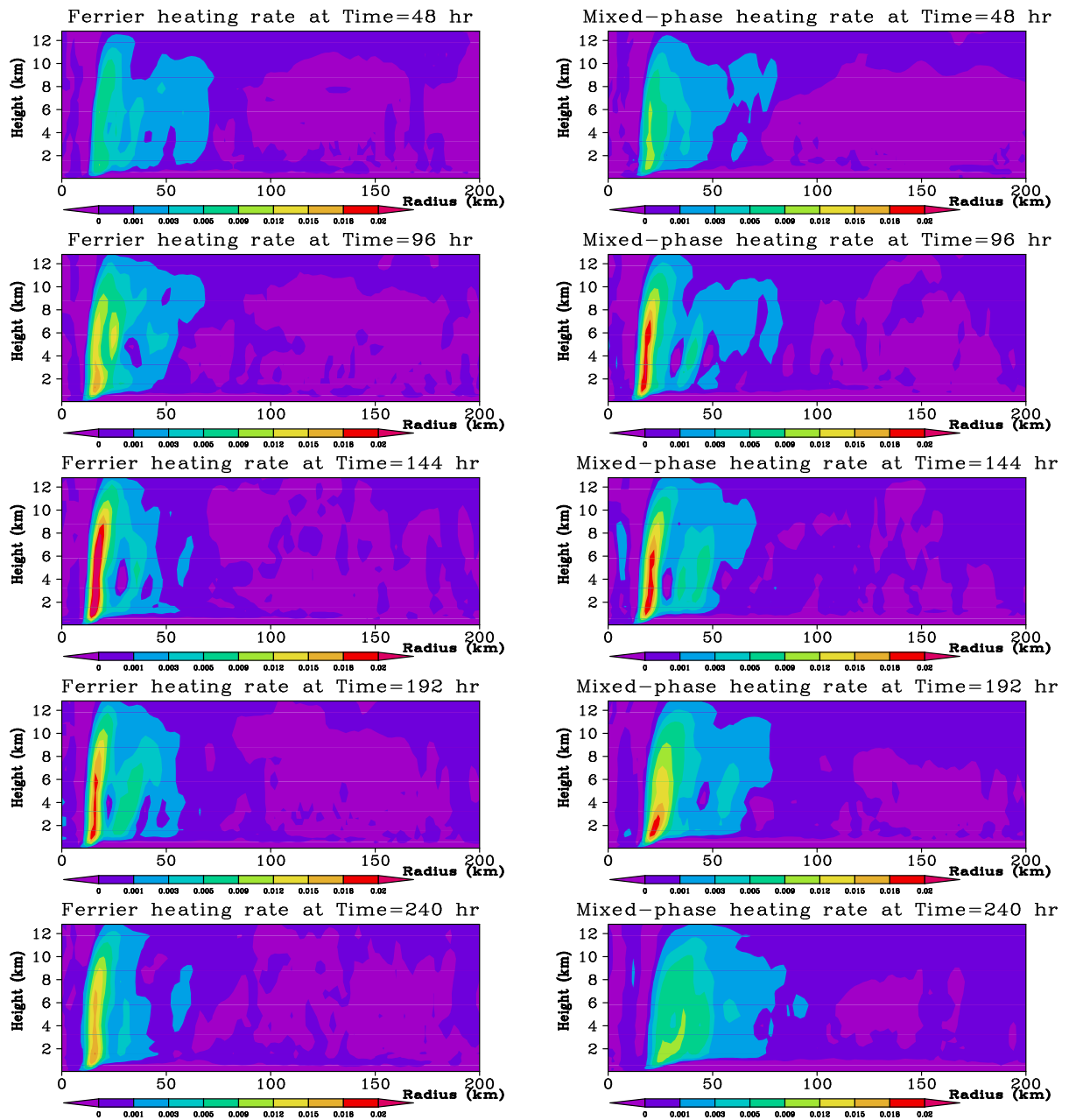


Figure 4. Radius-height distribution of the azimuthal mean diabatic heating at given times in the simulated storm with the Ferrier (left) and TCM4 (right) cloud microphysics schemes.

(a) Ferrier Scheme

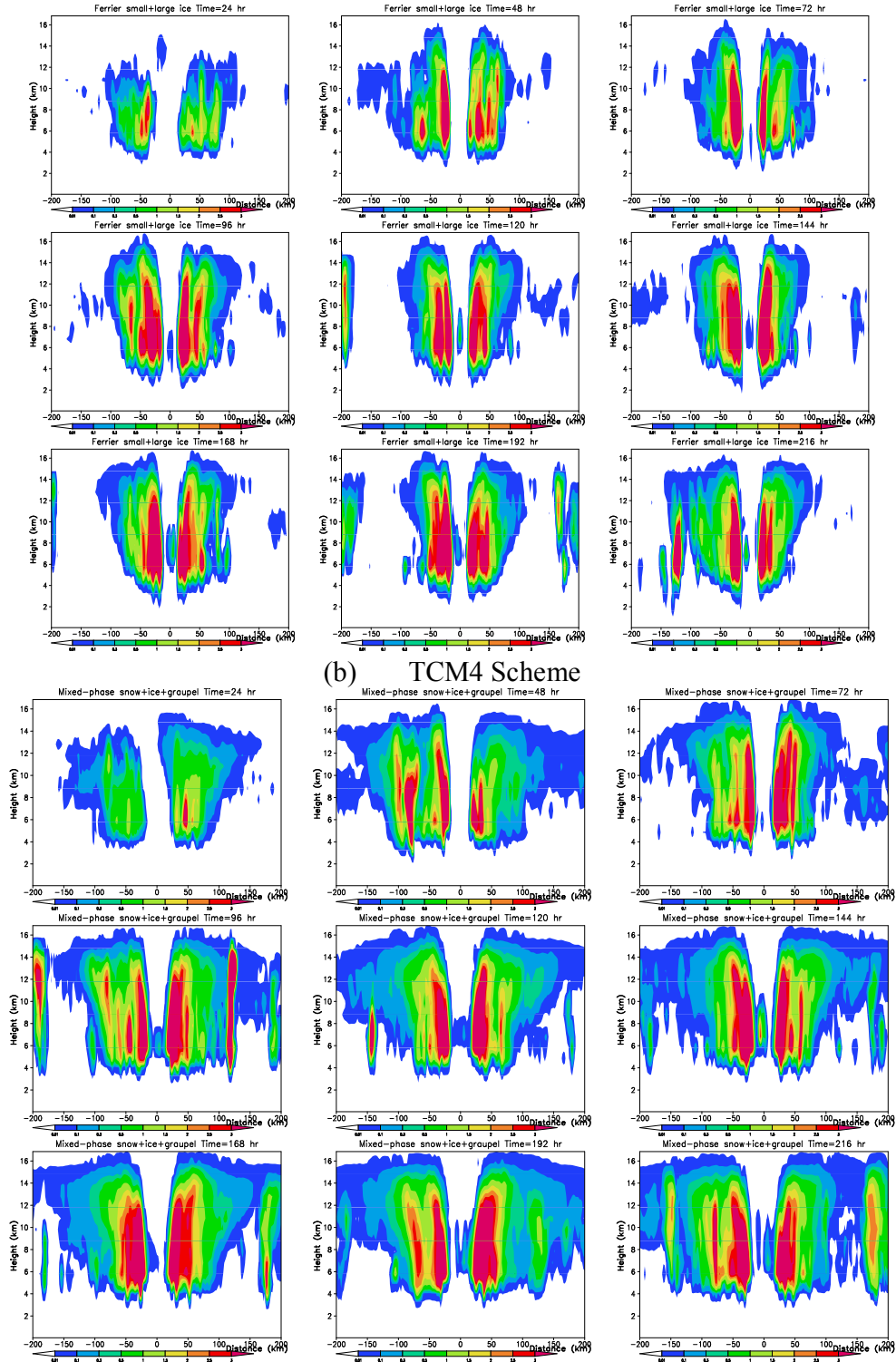


Figure 5. vertical cross-section of total ice along the east-west across the storm center simulated by Ferrier scheme (a) and TCM4 cloud microphysics scheme (b).
 b. Effect of the SAS cumulus parameterization scheme in TCM4

In order to examine the effect of the use of a convective parameterization scheme in the outer coarse meshes on the simulated hurricane structure and intensity, we have implemented the Simplified Arakawa-Schubert (SAS) cumulus parameterization scheme into TCM4 and performed two experiments using TCM4 with the finest mesh resolution of 2.5 km (note that a little bit coarser than that used for the simulations discussed above). Note that the SAS cumulus parameterization scheme is currently used in the operational HWRf model. In one experiment, the SAS cumulus parameterization scheme is used. Considering the horizontal resolution of TCM4, we only activated the SAS cumulus convection scheme in the two outer coarse meshes (with resolutions of 67.5 km and 22.5 km). In the other experiment, no any cumulus parameterization scheme is used in any model meshes.

Figure 6 shows the time evolution of the maximum azimuthal mean wind speed at the lowest model level and the minimum sea level pressure in the two simulations using TCM4. What we can see is the different evolutions of the storm intensity at some later stages while with little difference in the early intensification stage. This can be explained by the fact that the use of the cumulus parameterization in the coarse meshes takes time to affect the innermost mesh where most active convection occurs. Nevertheless, the differences still become visible and significant at later stages. In particular, the storm without the use of convective parameterization in the outer meshes becomes not only stronger and but also larger, as inferred from the radial distribution of rainfall rate shown in Fig. 7. The results from these sensitivity experiments thus demonstrated that the use of cumulus convective parameterization in the operational HWRf may need to be tested further. The interaction between the grid-scale and subgrid scale moist processes is also complicated. This is implicated further by the use of the implicit subgrid scale processes in different meshes in a nested model, such as the one used in the HWRf model.

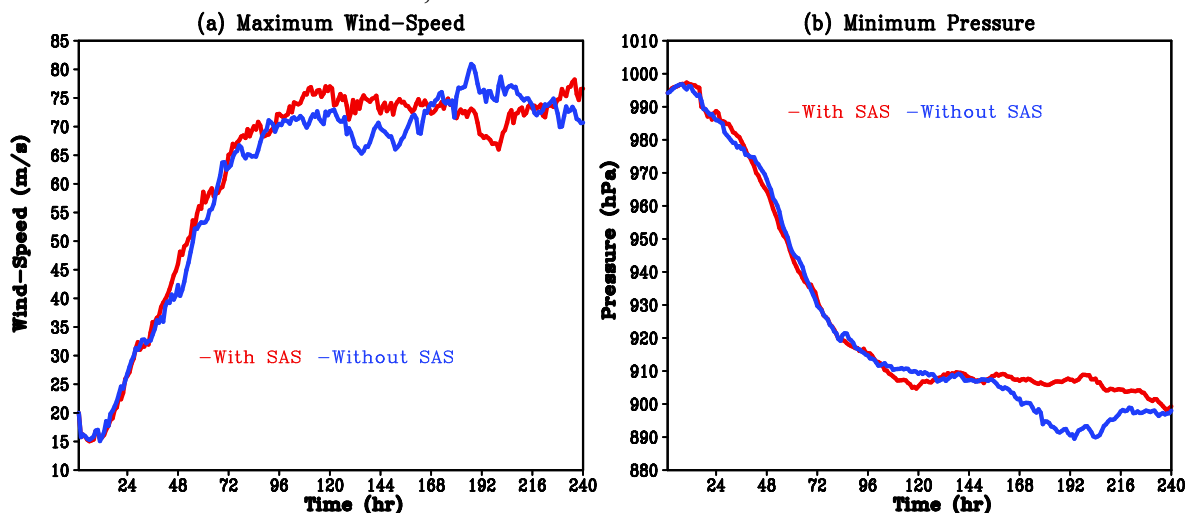


Figure 6. (a) The maximum azimuthal mean wind speed at the lowest model level (about 35 m above sea level); (b) the minimum sea level pressure of the simulated storms using Wang cloud microphysics scheme with (red) and without (blue) the use of the SAS convective parameterization scheme in the outer coarse meshes in TCM4.

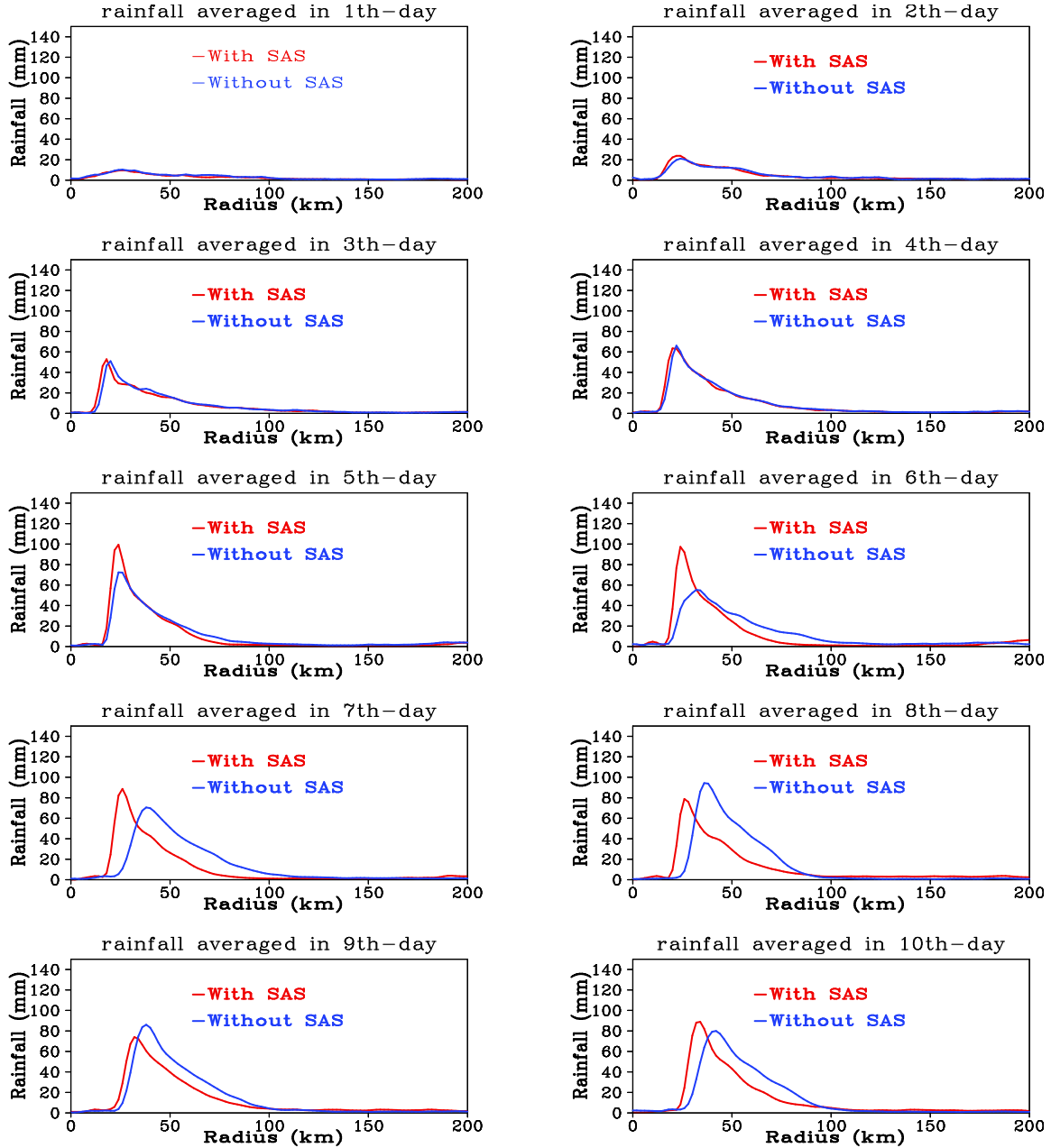


Figure 7. The azimuthal mean rainfall averaged in each 24h of simulations (red: with, blue: without the use of SAS convective scheme in the outer coarse meshes in TCM4).

c. Comparison of the NMM and ARW dynamical cores

We have extended our diagnostics of cloud and precipitation physics to examine the possible discrepancies in the dynamical core of the HWRF model in comparison with the simulation using the WRF_ARW dynamical core with the same model physics options. HWRF model is based on the dynamical core of the nonhydrostatic mesoscale model (NMM) of NCEP. WRF ARW dynamical core is developed at NCAR and is widely used in research and modeling

community. It is our purpose to see whether biases in the prediction of hurricane size and intensity by HWRF are related to the dynamical core. Hurricane Katrina (2005) was selected in this comparison since it was one of the most devastating natural disasters in the United States in the history.

The NCEP final analysis data (FNL) was used as both the initial field and boundary conditions. As we can see from Fig. 8 that hurricane intensity in FNL is generally considerably weaker, in particular during the mature stage, than that given in the NHC best track data. We therefore used a bogus scheme (Wang 2007) to enhance the initial hurricane intensity in FNL. The model domain was triply nested with grid spacings of 0.15, 0.05, 0.017 degree for NMM core and 15000, 5000, 1666.66 m for ARW core, roughly the same resolution for the two dynamical cores. The rapid intensification phase of Hurricane Katrina was covered by the finest model domain (not shown). To focus on the dynamical core, we used the same physics options in all experiments, namely, the physics schemes used in the operational HWRF at NCEP, including Ferrier scheme for grid-resolved cloud microphysics, Betts-Miller-Janjic (BMJ) scheme for cumulus convection, GFDL long/short-wave radiation scheme, Monin-Obukhov scheme for ocean surface flux calculation, the Noah land-surface model, Mellor-Yamada-Janjic (MYJ) TKE scheme for the planetary boundary layer (PBL). Convective parameterization was used only in the outermost domain. Three sensitivity experiments were conducted, namely NMM dynamical core without and with bogus vortex, and ARW dynamical core with bogus vortex. Note that the bogus vortex was embedded in the FNL only at the initial time. Therefore, except for different dynamical core (and also the pre- and post-processing), in the bogused experiments, the model physics and initial and boundary conditions were identical. This allows for a direct comparison of the two dynamical cores in the WRF modeling system.

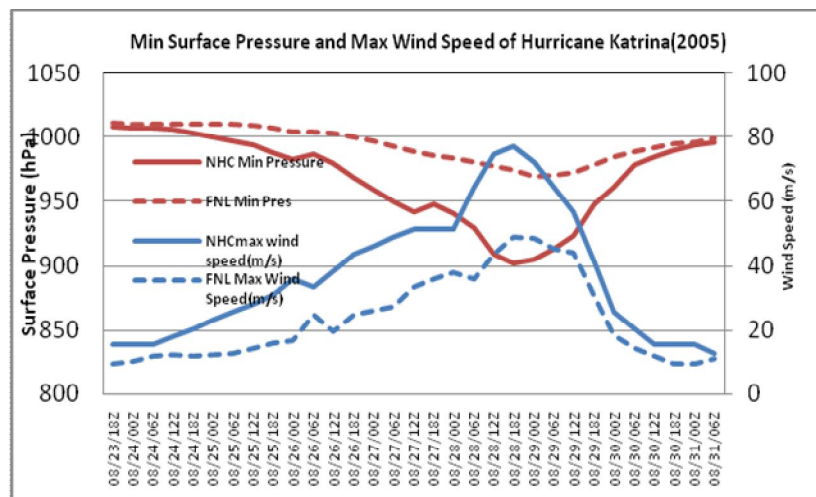


Figure 8. Minimum sea level pressure (purple) and maximum surface wind speed (blue) in the NHC best track data and in the NCEP FNL analysis.

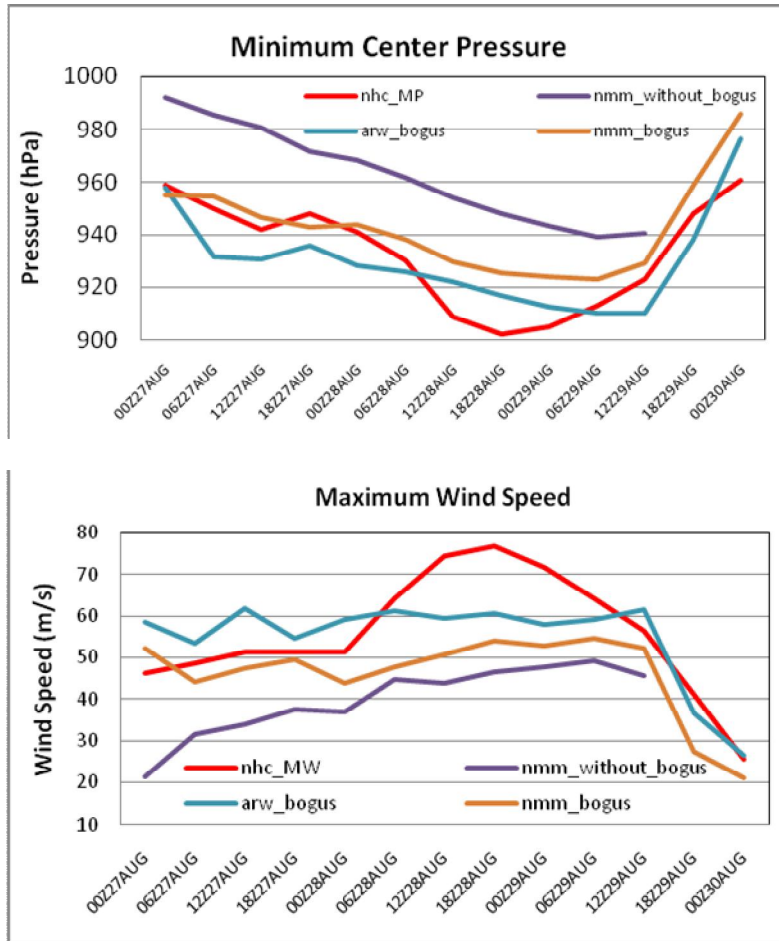


Figure 9. Minimum sea level pressure (upper panel) and maximum surface wind speed (lower panel) in the NHC best track, and from the three numerical experiments designed to examine the effect of dynamical core on the simulated storm by HWRF.

The initial intensity is very close to the observation in both simulations with vortex bogus (NMM_bogus and ARW_bogus in Fig. 9). Both captured the main intensity evolution of Hurricane Katrina but both failed to simulate the rapid intensification on August 28. The experiment without bogus scheme (NMM_without_bogus) also captured the intensity evolution except that the intensity is weaker than that with the bogus vortex. Note that although the same initial conditions were used in the two bogus simulations, the storm intensity immediately after the pre-processing had a higher maximum surface wind (about 10%) in the ARW dynamical core than in the NMM dynamical core. The storm simulated in the former was also considerably stronger than that in the latter. The simulation with the NMM dynamical core without bogus vortex reproduced the intensification better than that with the bogus vortex, indicating that the NMM dynamical core might not be able to simulate very strong intensity of hurricanes. Note that although we show only simulations at one initial time, experiments with different initial times gave quite similar results (not shown). Therefore, in terms of storm intensity prediction by

HWRP, two aspects need to be addressed, why the initial surface wind speed of the storm is weak and why the simulated maximum surface wind intensified much slower than the central surface pressure deepened. All three simulations captured the storm motion reasonably well (Fig. 10). Although the storm in the experiment with no bogus vortex in NMM_without_bogus is much weaker than that with the bogus vortex (NMM_bogus), the simulated tracks in the two experiments were quite similar (not shown). Further, although the NMM dynamical core simulated weaker hurricane intensity, it simulated the track considerably better in terms of the landfall timing and location than the ARW dynamical core for this case. This indicates that the NMM dynamical core might capture the evolution of the large-scale environmental flow, which is the key to the accurate prediction of storm motion. However, the storm intensity is largely controlled by the inner core dynamics, which was not well represented by the numerical scheme and needs to be improved in the NMM dynamical core.

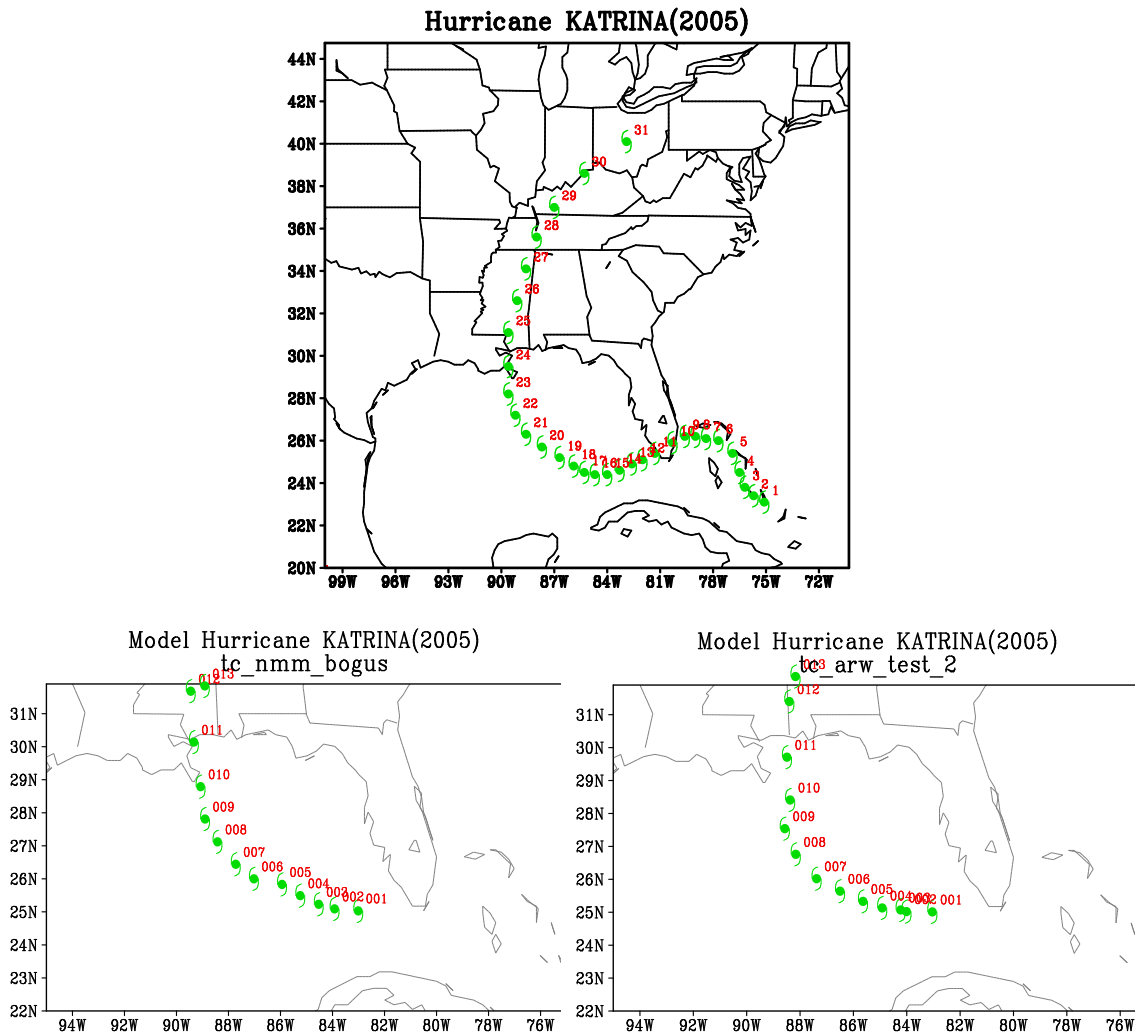


Figure 10. The best track of Hurricane Katrina (2005) from the NHC best track data (upper panel) and that predicted by WRF model with NMM (lower left) and ARW (lower right) dynamical core.

Figure 11 shows the height-radius cross-section of the azimuthally mean tangential wind at the initial time and after 24 h simulation from two experiments with bogus vortex. Consistent with the intensity evolution shown in Fig. 9, at the initial time, the azimuthal mean tangential wind is already weaker throughout the depth of the troposphere in the NMM dynamical core experiment. The difference at the initial time is purely a result of the different pre-processing algorithms used in the two dynamical cores. After 24 h of simulation the difference became even larger. In particular, the NMM dynamical core simulated a shallower maximum tangential wind core immediately above the boundary layer around 850 hPa while the ARW dynamical core produced a maximum tangential wind core extending to higher levels. This difference might be related to the difference in the vertical discretization of the two dynamical cores. In addition, the radius of maximum wind in the lower troposphere is also larger in the simulation with the NMM dynamical core than that with the ARW dynamical core, indicating that the dynamical core also contributes to the too large storm in the prediction of hurricanes by the HWRF. We have tested the effect of divergence damping used in the NMM dynamical core and found that it affects the simulated size of the storm but it seems not the main reason. Therefore, a systematic dynamics of dynamical core of the NMM is required in order to improve the prediction of storm intensity and structure by HWRF. Here we have only highlighted its potential impact on the model prediction.

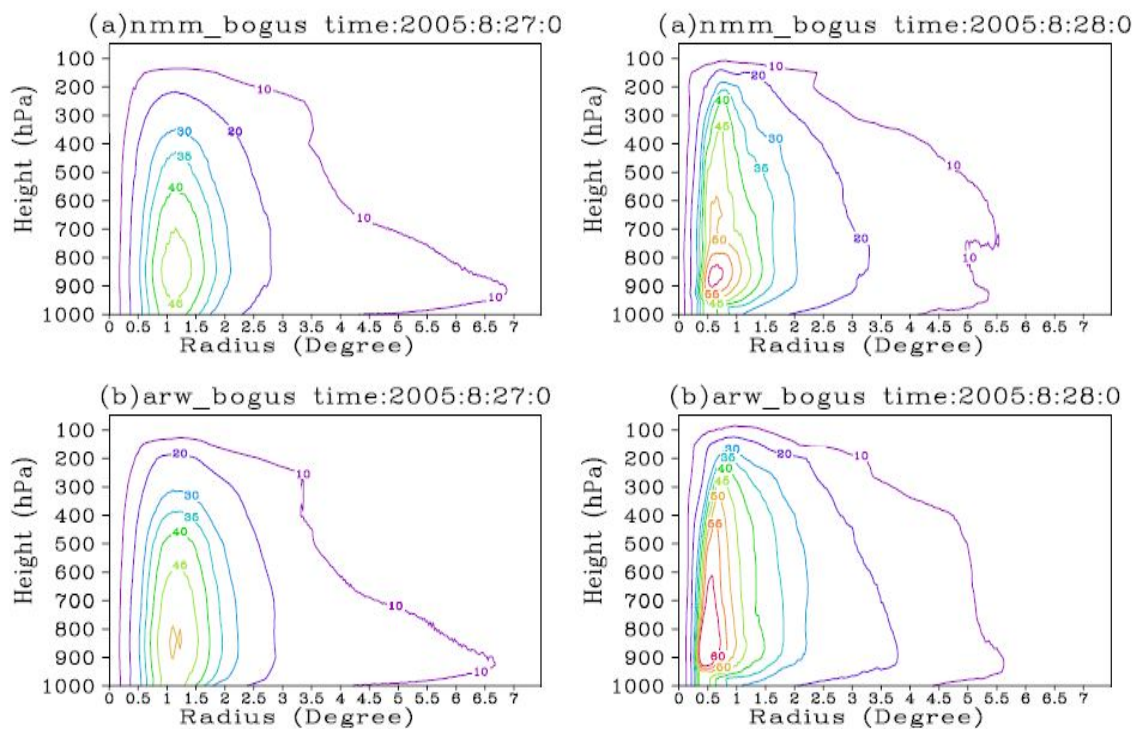


Figure 11. Height-radius cross-section of the azimuthally mean tangential wind at the initial time and after 24h of simulation with the NMM and ARW dynamical core and the initial bogus vortex.

Corresponding to the difference in the vertical structure of the simulated azimuthal mean tangential wind shown in Fig. 11, the warm core, defined as the temperature anomaly related to annulus mean temperature between radii of 500 km to 750 km, is similar at the initial time but became stronger in the simulation with the ARW dynamical core (Fig. 12), consistent with the stronger storm in the simulation than that in the NMM dynamical core experiment. Larger negative temperature anomalies occurred in the simulation with the ARW dynamical core than that with the NMM dynamical core, indicating that not only the physics parameterizations can affect the heating/cooling distributions but also the dynamical core may affect how the dynamics responds to the physical forcing in hurricane simulations. Furthermore, even the same cloud microphysics scheme was used in the two simulations the distribution of hydrometeors is quite different. An example of the azimuthal mean radius-height distribution of cloud water is given in Fig. 13. We can see that the cloud liquid water shows shallow clouds outside the eyewall and extends outward to large radii in the lower troposphere, indicating shallow clouds above the boundary layer. This can explain why the negative temperature anomalies are so small in the lower troposphere in the simulation with the NMM dynamical core. In addition, the cloud water also fills in the lower eye region in the simulation with the NMM dynamical core. These results suggest that the dynamical core may affect the cloud microphysics to some degree. This has never been recognized.

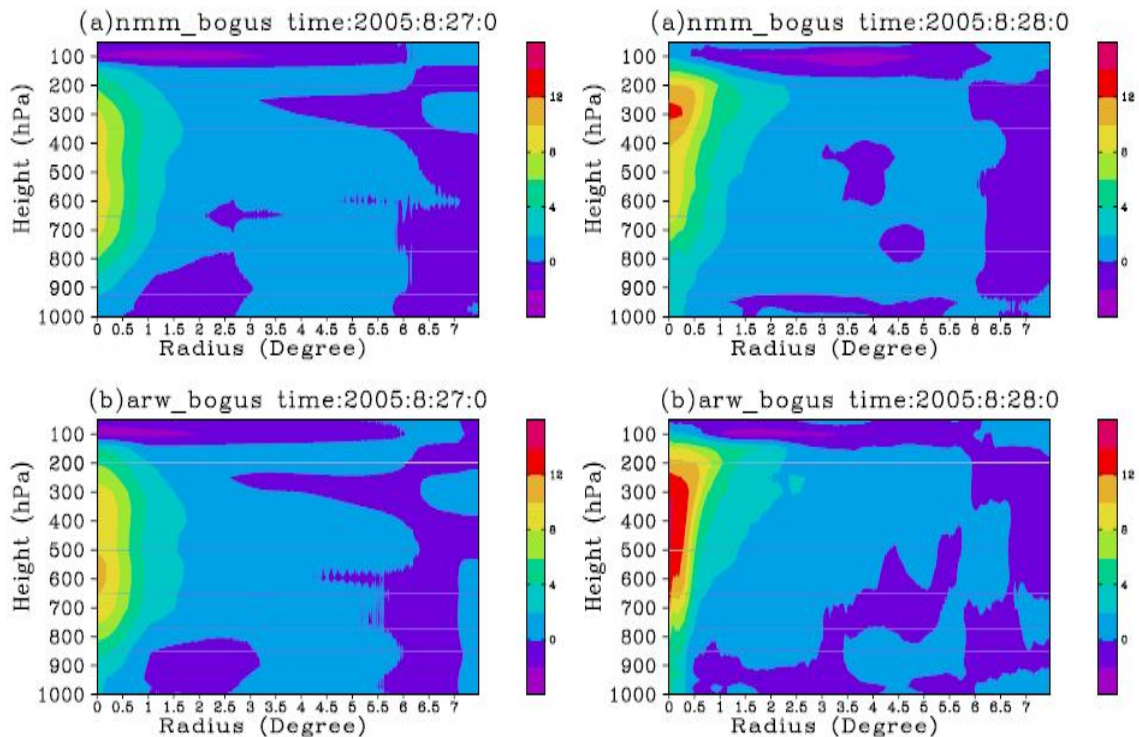


Figure 12. Height-radius distribution of the azimuthally mean temperature anomalies at the initial time and after 24 h of simulation with the NMM and ARW dynamical cores and initial bogus vortex.

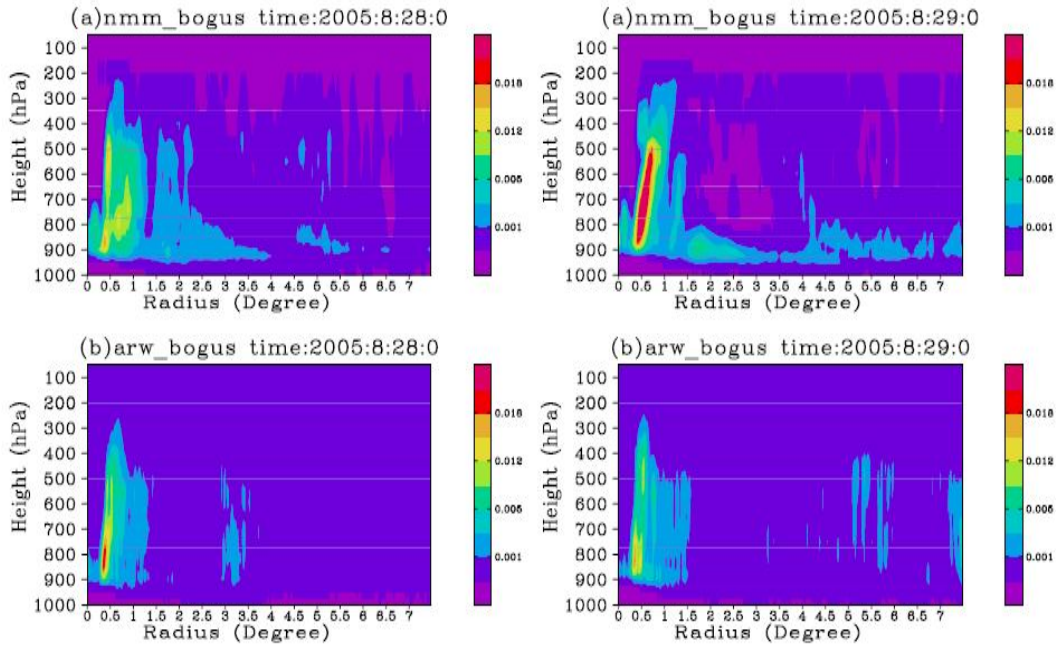


Figure 13. Height-radius distribution of the azimuthally mean cloud water after 24 h and 48h of simulations with the NMM and ARW dynamical cores, respectively.

d. Development and test of the SCPM

In accordance with the work-plan of the project, during Year 1 we have developed and tested a single-column parcel model (SCPM). Later in this project, this SCPM will have two roles for improving forecasts with the HWRF model:

- Provide improved parameterization of supersaturation and other microphysical quantities (e.g. liquid fraction) assumed to treat the grid-resolved clouds;
- Embed the SCPM inside the deep convection parameterization, providing better estimates of convective heating aloft and detrainment of condensate mass.

To minimize computational expense, our SCPM represents an adiabatic parcel with a simplified cloud-microphysical framework. It treats coagulation of hydrometeors with the single-moment bulk microphysics scheme described by Phillips and Donner (2006). There are 5 classes of hydrometeor: cloud-droplets, cloud-ice, rain, snow and graupel. In the SCPM, cloud does not sediment, while precipitation does. Diffusional growth of cloudy condensate is treated by applying the formula from Korolev and Mazin (2003) for the supersaturation, as a function of cloud-liquid and cloud-ice properties. The change in supersaturation during ascent from one model level to the next determines that of all cloud condensate due to diffusional growth, which constrains the individual rates of condensation and vapor growth of cloud-liquid and cloud-ice. Cloud-droplets and cloud-ice particles are assumed to be monodisperse, with number mixing ratios that are 10^8 and 10^5 kg^{-1} respectively below the -36°C level, being zero and 10^8 kg^{-1} respectively above due to homogeneous freezing.

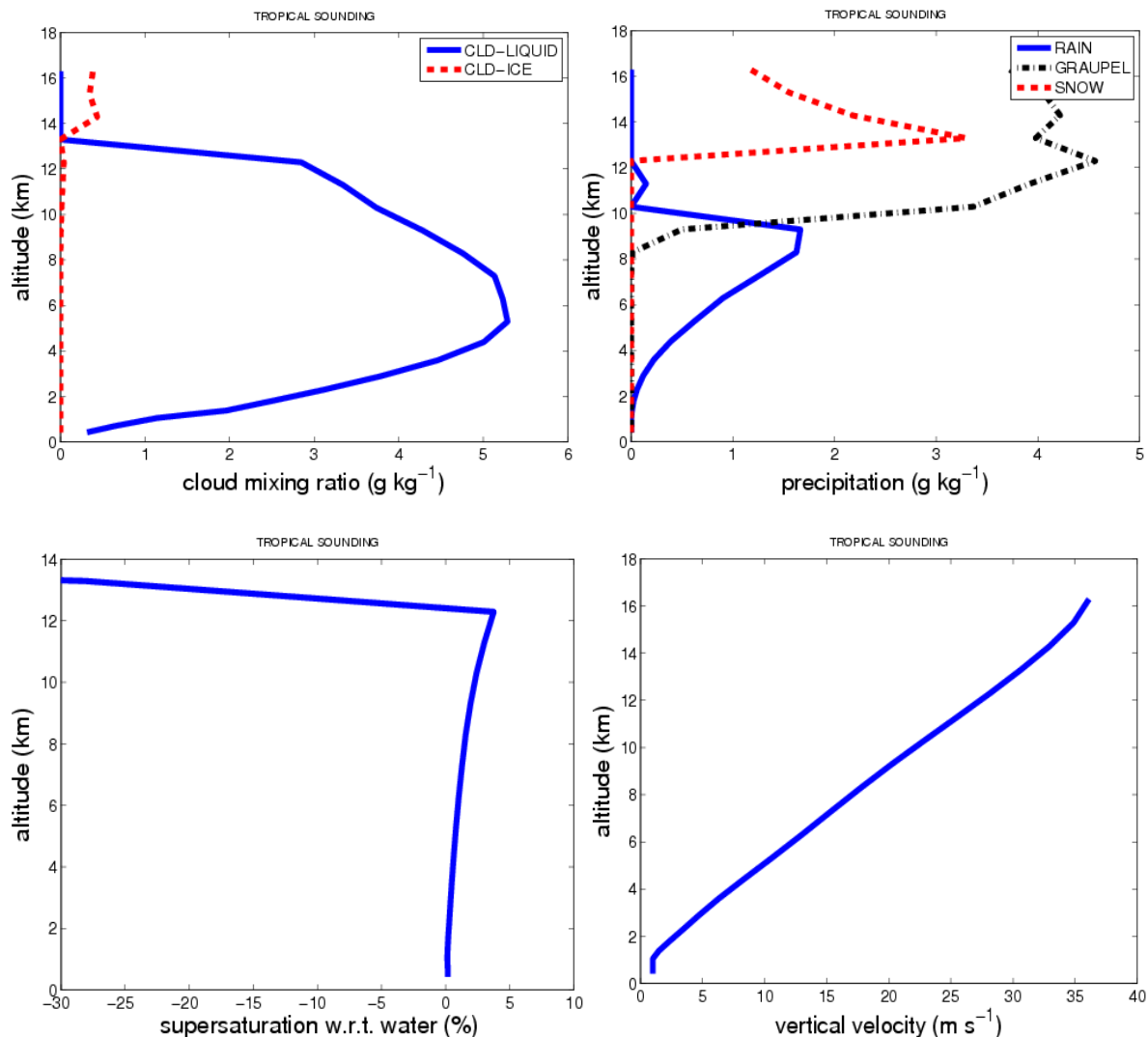


Figure 14. Off-line simulation by the SCPM of a cloudy adiabatic parcel in a vigorous deep convective updraft, for an unstable sounding. The depth of the parcel is 1 km and the ascent is calculated from an extremely unstable tropical sounding, with a relative humidity of 86% and air temperature of 27° C near the surface, and a convective available potential energy (CAPE) of about 6000 J/kg. To integrate the evolution equation of parcel kinetic energy, it was assumed that 10% of the CAPE was converted to kinetic energy of the parcel, implicitly accounting for the effects of other retarding factors (e.g. gravitational burden of condensate, vertical perturbation pressure gradient force). Note the discontinuity of supersaturation at the top of the mixed phase region (about 12 km altitude). There, all supercooled cloud-liquid upwelled there must freeze, causing a collapse of humidity to ice saturation.

First, after developing the SCPM, it was tested for a tropical case of a convective ascent in a very unstable atmosphere. Figure 14 shows off-line results from the SCPM's simulation of a real tropical sounding that has extreme instability. Much of the rain is predicted to freeze, forming copious graupel in the mixed-phase region (0 to -36 degC). Thus, the SCPM

realistically captures a feature of convective updrafts found in other more detailed models, about graupel dominating the overall mass of ice precipitation. As is evident from Fig. 14, the SCPM realistically represents homogeneous freezing of all cloud-liquid at the level where the parcel reaches -36 degC (about 12 km altitude). Here, the humidity collapses during ascent towards ice saturation. The mass of cloud-ice becomes appreciable.

The SCPM represents how the supersaturation is maintained close to water saturation by an approximate balance between the adiabatic cooling from ascent and condensation, in this mixed-phase region, while the liquid fraction is close to unity. This is because of ascent is appreciable and the ice concentration is low in the mixed-phase region (see Korolev and Mazin 2003; Korolev 2007). Also apparent from Fig. 14 is the prediction by the SCPM of the inexorable increase of supersaturation with height in the deep convective updraft. This is partly due to the increasing rate of ascent and partly due to accretion of cloud-liquid. In natural convective clouds, this rise in supersaturation is an important feature, causing in-cloud droplet activation that tends to maintain the droplet number concentration at appreciable values, despite losses by accretion.

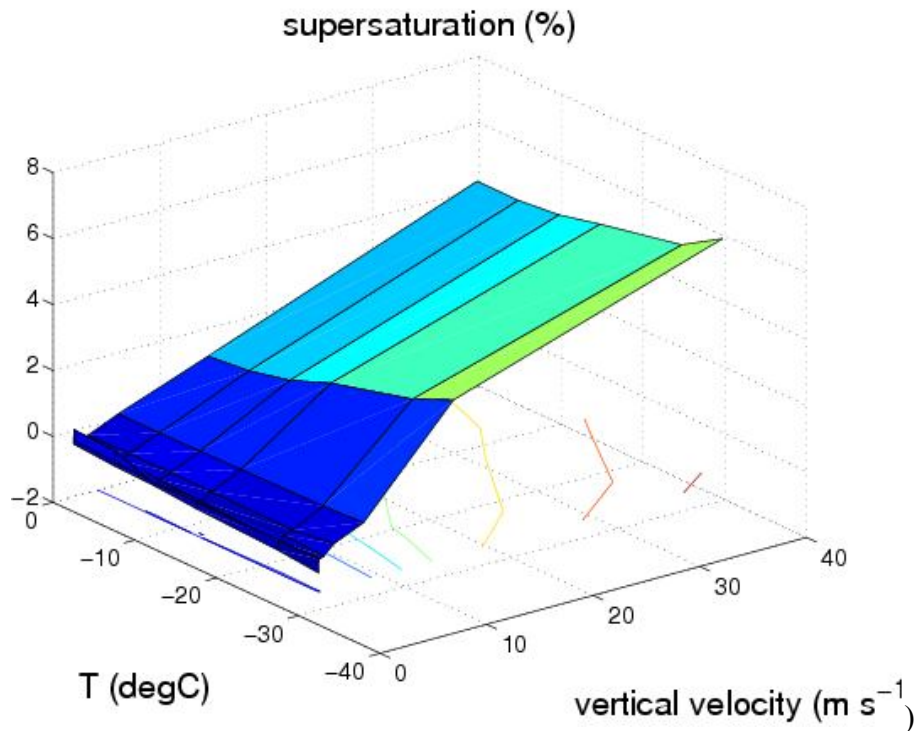


Figure 15. In-cloud supersaturation with respect to liquid water in an adiabatic parcel, predicted by many off-line runs of the SCPM. All parcel runs begin at the surface with relative humidity of 86% and temperature of 27°C . Ascent is prescribed at a constant value during each run. Note how the faster the ascent, the greater the supersaturation. Accretion of cloud by precipitation explains why the supersaturation does not decrease markedly with increasing supercooling. The absence of negative supersaturations here is consistent with findings of Korolev (2007) and Phillips et al. (2007) about the Bergeron-Findeisen process being usually restricted to weaker ascent, depending on the ice concentration.

Next, many idealised runs were performed with the SCPM, in order to create enhanced microphysical parameterisations for the hurricane model. Vertical velocity was prescribed at a fixed, constant value in each run. Different rates of ascent were assumed in different runs. Figure 15 shows the supersaturation in the mixed-phase region, from this ensemble of idealised runs. Liquid fraction is predicted to be close to unity for most of the vertical velocities of these runs. The plotted results (Fig. 15) form a look-up table that may be applied to treatments of both large-scale stratiform and convective clouds in the hurricane WRF model.

During Year 2 of the present project, in addition to applying it to improve the hurricane model, as noted above, development of the SCPM may make use of our recent codes for bulk microphysics in an aerosol-cloud model (Phillips et al. 2007, 2009). There may be improved conversion of cloud-ice to snow, sub-cycling for coagulation processes when ascent is slow, and more accurate cloud-ice numbers in the mixed-phase region. During this Year 1, this bulk microphysics code of the aerosol-cloud model has been improved with emulated bin microphysics to represent the dependency of ice morphology (shape, bulk density) on size, for graupel and snow. Simple theoretical formulae to predict cloud-droplet concentrations, due to in-cloud activation, have been derived by the Co-I, with analysis of in-cloud microphysical equilibrium. These all provide potential avenues for enhancing the SCPM during Year 2.

Second project year (08/01/2009-07/31/2010)

e. Effect of initial vortex size on the predicted storm inner-core size change

The influence of the initial vortex size on the inner-core size of the simulated hurricane has been investigated using TCM4. We have focused on how the initial vortex size (the radius of maximum wind-RMW) controls the hurricane inner-core size in the mature stage. A positive feedback mechanism responsible for the hurricane inner-core size is identified (Xu and Wang 2010). Figure 16 shows the radial profiles of the tangential wind and vertical relative vorticity in the initial vortices used in our numerical experiments. Here the profiles from S40 to S100 indicate the increase in the initial RMW from 40 km to 100 km. What we can see here is that the larger vortex shows large cyclonic relative vorticity up to a radius beyond 200 km while the small vortex has cyclonic relative vorticity in a radius less than 100 km. As a result, the large vortex has its high inertial stability to extend to larger radii, which prevents the boundary layer inflow due to friction and diabatic heating in the eyewall. This leads to a slower intensification of the storm in the subsequent model simulation. In sharp contrast, the small vortex intensified faster but reached a weaker intensity at its mature stage, as we can see from Figure 17. One interesting result is that the small storm remained small throughout the integration while the large storm increased its inner core size considerably with time (see Figures. 18 and 19). To understand the model storm behavior, we have elaborated a positive feedback between the storm size and the convection outside the eyewall as documented in Xu and Wang (2010).

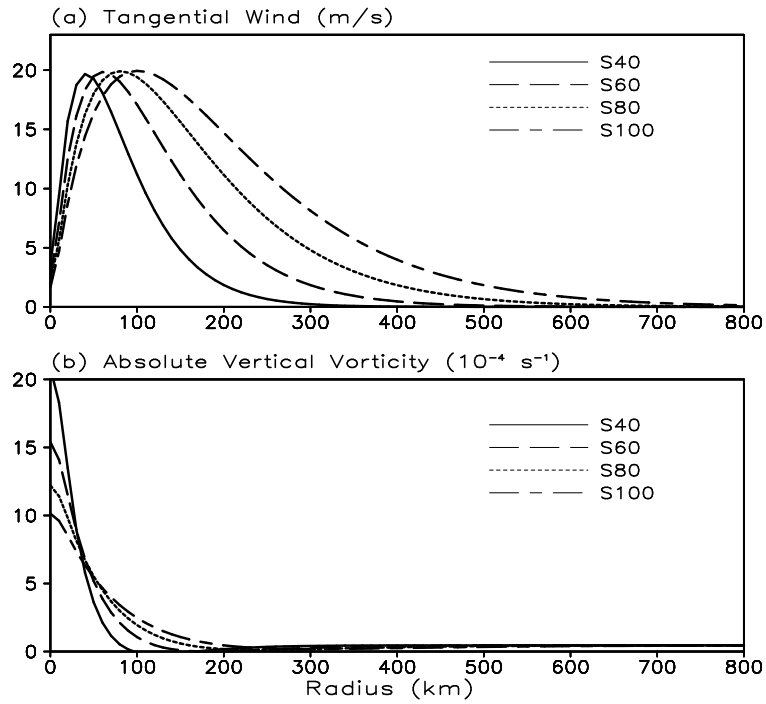


Figure 16. The radial profiles of the tangential wind (a) and relative vorticity (b) used in the sensitivity experiments using TCM4 to understand how the size change varies with the initial vortex size.

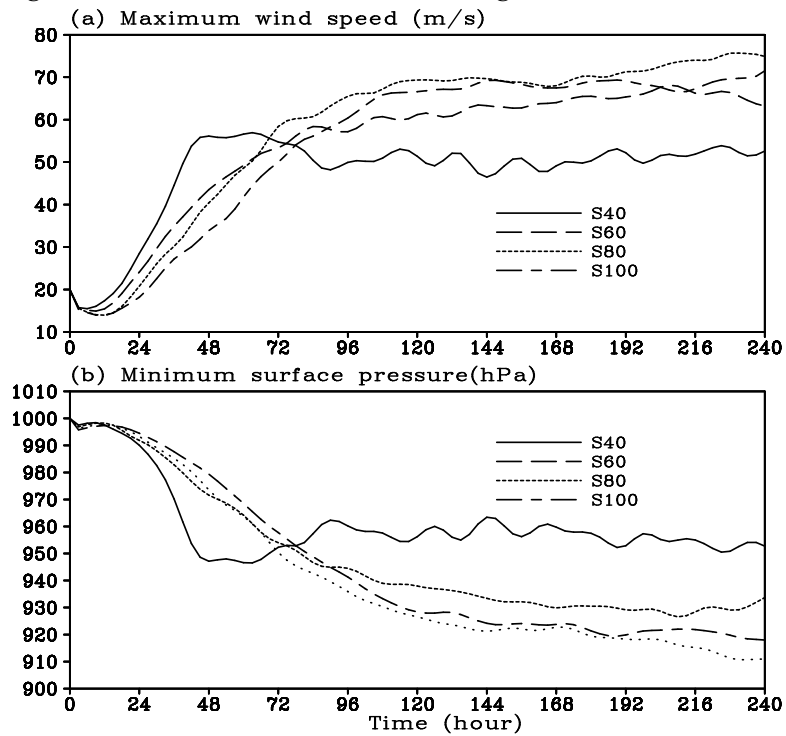


Figure 17. Time evolution of the maximum wind at the lowest model level (a) and the minimum central sea level pressure (b) in the four experiments using TCM4.

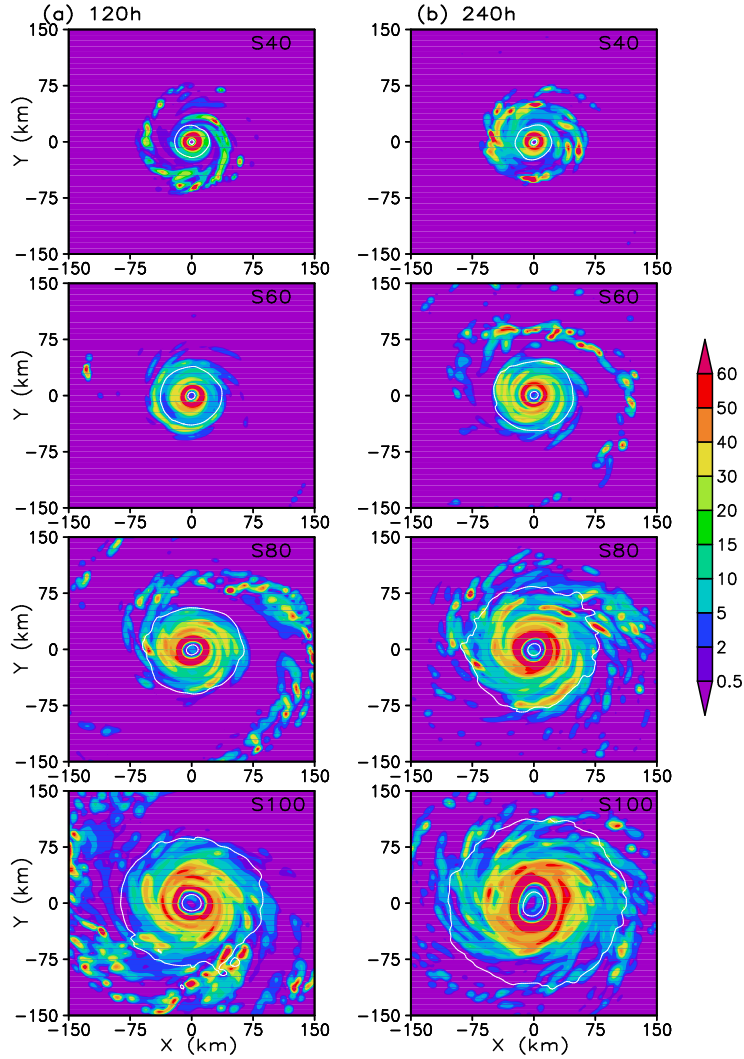


Figure 18. The TCM4 simulated surface rain rate in 4 experiments for the four storms with different initial size as shown in Figure 17 after 120 h (left column) and 240 h (right column) of simulation.

We found that a large initial size vortex has a broad tangential wind distribution outside the RMW, causing large surface entropy fluxes outside the eyewall and favoring the development of active spiral rainbands. Diabatic heating in spiral rainbands drives strong boundary layer inflow outside the eyewall. The latter brings high absolute angular momentum inward and thus contributes to the increase in tangential winds outside the eyewall, leading to the outward expansion of the wind field and the increase in the inner-core size of the simulated hurricane.

The broadened wind field in the initially large storm favors more surface entropy flux outside the eyewall and thus more active spiral rainbands. In addition, the large radial extent of relatively high absolute vertical vorticity (and thus the large inertial stability) in the large-size initial vortex makes the increase in tangential wind due to radial advection of absolute angular momentum effective. This is a positive feedback for the large initial size vortex to increase in its

inner-core size in the simulation. On the contrary, a small initial size vortex with the same intensity has weak winds and thus small surface entropy fluxes outside the eyewall, prohibiting the development of active spiral rainbands in large radii, resulting in weak boundary layer inflow outside the eyewall and limiting the radial advection of absolute angular momentum. As a result, the increase in tangential winds outside the eyewall is suppressed, the outward expansion of the wind field is prohibited, and thus the inner-core size remains small (Figures 18 and 19). This is a positive feedback to maintain a small inner-core size storm. The positive feedback mechanism identified here can thus explain the observational results of Cocks and Gray (2002), which showed that small TCs were smaller than the medium and large TCs early on and throughout their respective composite lifecycles. The results also strongly suggest that the rapid size increase of hurricane in the HWRF model might be related partly to the initial vortex size in the initialization scheme. In addition, the model resolution at 9 km might be a reason too since at this resolution the model could not resolve the observed RMW. As a result, higher resolution may be needed in order to improve the size prediction by the HWRF model.

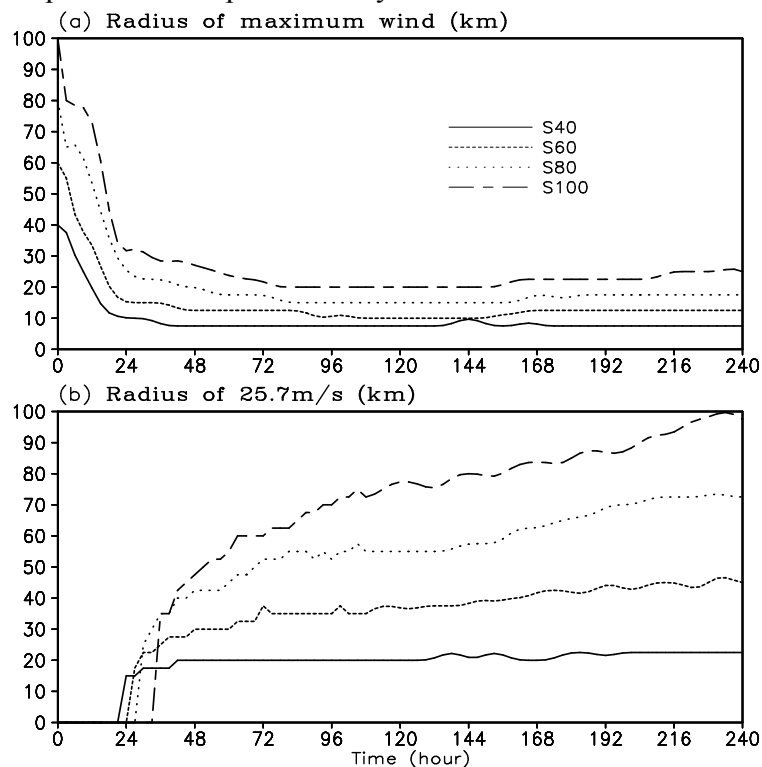


Figure 19. Time evolution of the radius of maximum wind (a) and the radius of damaging wind (b) in the four experiments using TCM4 with different initial vortex size shown in Figure 17.

f. Sensitivity of the predicted storm size change to the initial radial wind profile

The above explanation as a positive feedback to lead to size change in the simulation can be further tested by using the initial vortices with the same radius of maximum wind while varying the radial decaying rate of the initial radial wind profile. We thus want to address how the radial

wind profile of the initial vortex may affect the subsequent size evolution in the model integration. To address this issue, we performed three more experiments with the initial vortices having the same radius of maximum but different radial decaying rate outside the RMW as shown in Figure 20. Similar to the vortices specified in the initial size experiments, here the vortices show different extension of cyclonic relative vorticity outside the core region (Figure 20b). For the broad vortex, winds are strong outside the eyewall with relatively higher relative vorticity extending outward up to 300 km, while the compact vortex have cyclonic vorticity in about 200 km radius. This difference presents difference in inertial stability and also implies higher surface entropy flux for broad vortex as the case shown earlier for large size vortex. As a result, the mechanism and evolution of the size change for the different shapes of the initial vortex are similar to those discussed for the dependence on the initial vortex size (Figures 21 and 22).

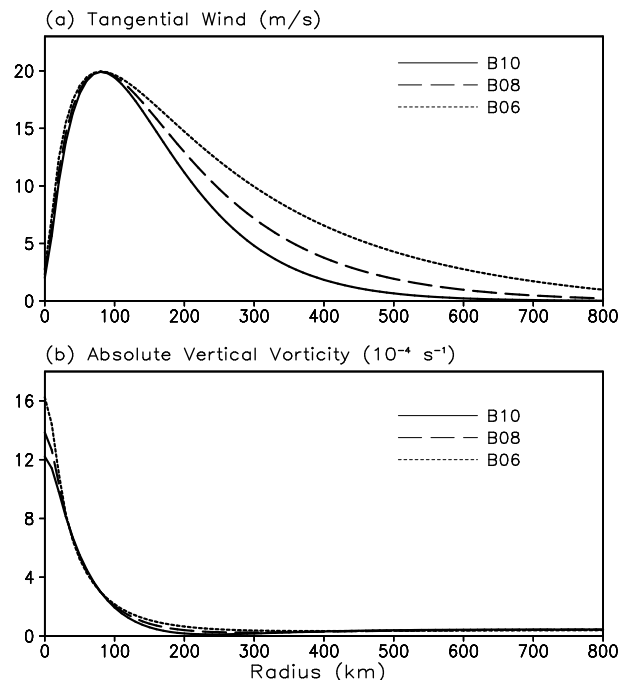


Figure 20. The radial profiles of the tangential wind (a) and relative vorticity (b) used in the sensitivity experiments using TCM4 to understand how the size change varies with the initial vortex size.

g. Setup of a real-time forecast system for the western North Pacific

During this reporting period, we have mainly focused on the configuring and testing the newly released HWRF model V3.3 (to have replaced its interim version). To allow us to evaluate the HWRF model in a quasi-operational context, we have set up the HWRF model in a real-time forecast mode at University of Hawaii and configured it to the western North Pacific. Currently we are testing the real-time system and it is working reasonably well after some problem shootings. It is much complicated as originally expected for a real-time forecasting system indeed.

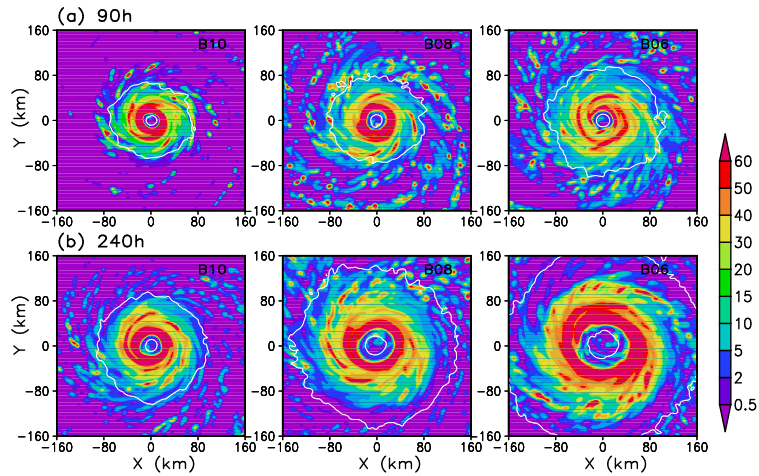


Figure 21. The TCM4 simulated surface rain rate in the 3 experiments for the storms with different initial shape in their radial profile of tangential wind as shown in Figure 20 after 90 h (top panel) and 240 h (lower panel) of simulation

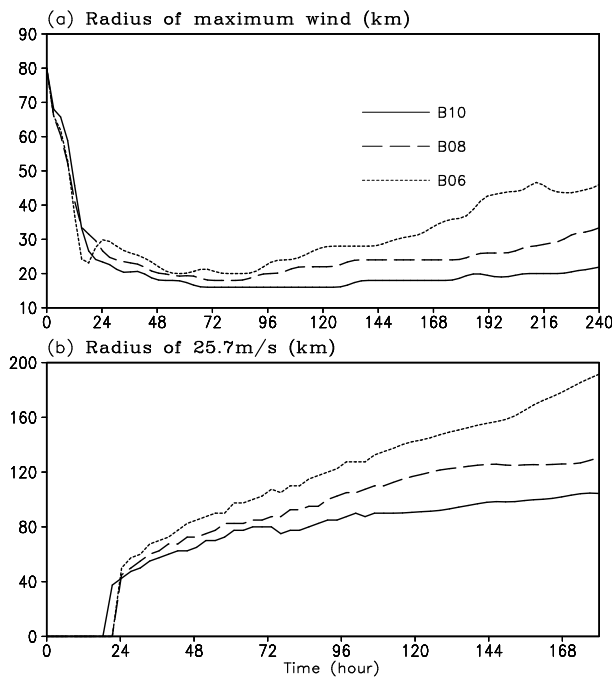


Figure 22. Time evolution of the radius of maximum wind (a) and the radius of damaging wind (b) in the three experiments using TCM4 with different radial wind profiles in the initial vortex size shown in Figure 20.

We have experiencing two major problems. Firstly, the initial vortex in the GFS analysis is too weak compared to the observations. This makes it difficult to verify any forecast of the model in its performance. Different from storms over North Atlantic, for storms over the eastern North Pacific and Central Pacific there are no aircraft observations. Therefore data assimilation

could not sufficiently improve the initial storm structure and intensity in any numerical models for the region. In amend this discrepancy, we constructed a balanced bogus vortex scheme initially to allow an enhancement of the initial storm in the model initialization and tested it in the western North Pacific this year using the ARW-WRF model. We have run the model in real-time for the whole tropical cyclone season this year and gained very useful experience in this sense. The model forecast is automatically displayed online in the International Pacific Research Center at University of Hawaii at <http://iprc.soest.hawaii.edu/users/dhcha/>.

Our initial evaluation of this bogus scheme indicates that this balanced vortex scheme only includes the axisymmetric vortex without a secondary circulation and it needs some time to be adjusted to the model dynamics and physics. Although it works reasonably well this year so far, a more dynamically consistent initialization is urgent and has been attempted by my group as discussed below.

h. Development of a new dynamical tropical cyclone initialization scheme

Now we have developed a new dynamical initialization scheme, which includes a relocation of the analyzed vortex in GFS at $t=-6$ hr and integration of the model for 6 hr to $t=0$. The vortex after this 6 hr integration is then relocated to the location of the observed storm at $t=-6$ hr. This is followed by a similar integration-relocation to form a dynamical cycle until the model storm having an intensity within 2 m/s of the observed storm at $t=0$. The model then performs a 120 hr forecast. Figure 23 shows the flow chart of the system.

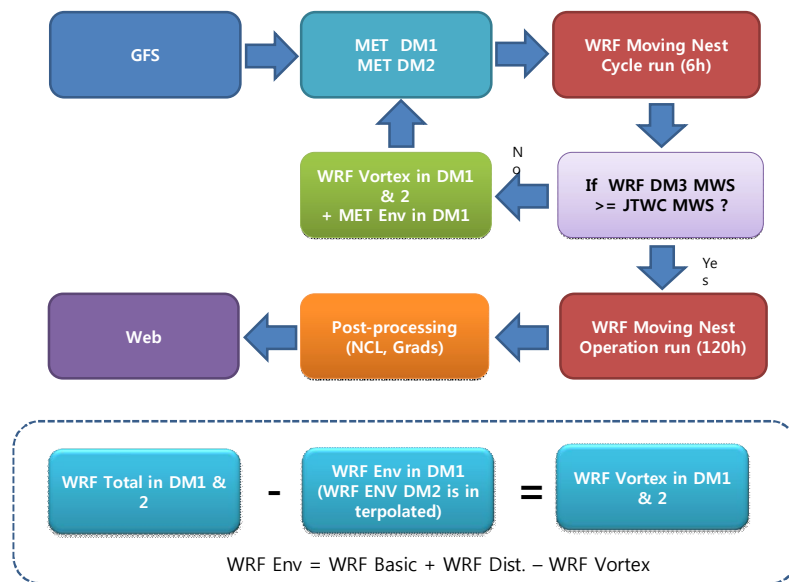


Figure 23. The flow chart of the real-time forecast system with the forecast cycling dynamical initialization and relocation.

An example of the dynamical Initialization for Moving 3 Nesting meshes

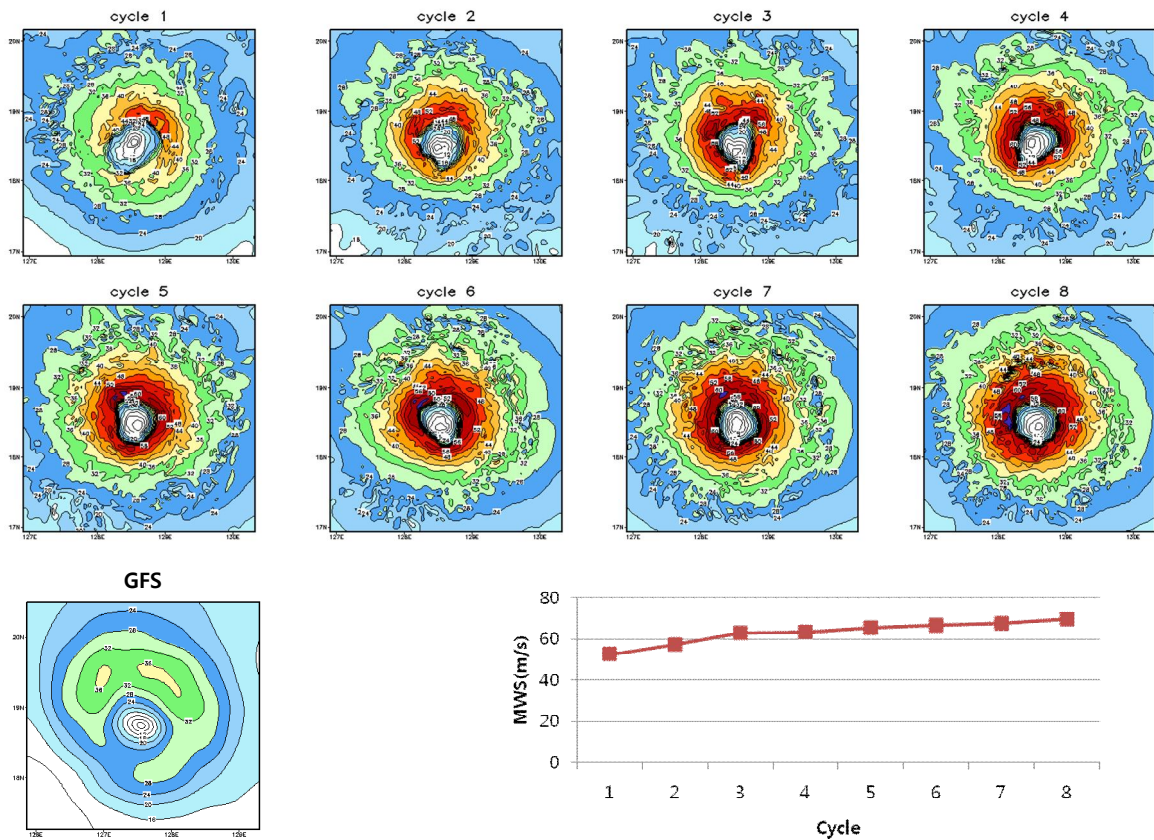
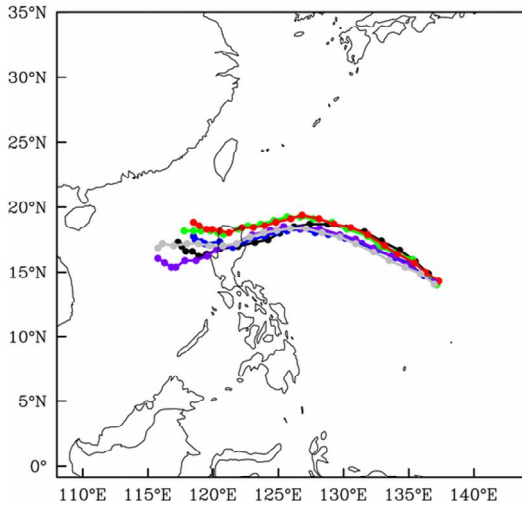


Figure 24. 10-m wind speed field in the innermost nested domain from the GFS analysis and from each cycle for Typhoon Megi (2010).

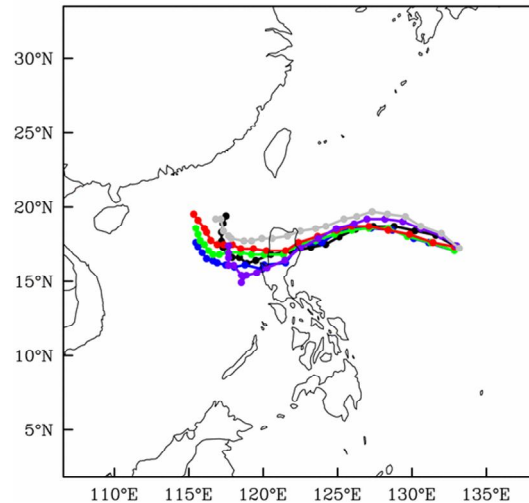
We show in Figure 24 the 10-m wind for Typhoon Megi (2010) over the western North Pacific as an example. We can see that the storm in GFS analysis is too weak compared with the observed maximum surface wind of about 70 m/s. Through the dynamical cycling, the storm intensified after each of the cycles and reached the observed intensity in the maximum surface wind after 8 cycles. In addition to the storm intensity, the dynamical initialization we developed also improves the 3-dimensional structure of the storm greatly (not shown). These indicate that the dynamical initialization scheme we developed is very efficient to improve the initial conditions for model tropical cyclones. To demonstrate the performance of the model in predicting tropical cyclone track and intensity, we show in Figures 25 and 26 the results from three forecast experiments for Typhoon Megi with the initial condition from GFS analysis while the lateral boundary conditions are from GFS forecasts. We can see that the accuracy of the track forecast strongly depends on the initial time for the Megi case. The earlier prediction seems the best in predicted landfalling location and the northward turning after the storm entered the South China Sea after across the Luzon Island. The model predicted northward turning is sensitive to the model resolution, the bogus vortex, the dynamical initialization scheme, and the different

physical parameterization schemes. The forecast intensity also varies with different physical parameterization schemes and different initialization schemes used (Figure 26). Nevertheless, the best intensity forecast comes from the dynamical initialization scheme. This demonstrated that the new dynamical initialization scheme we developed is a good approach to improve the initial conditions for HWRF model. This will allow us to further evaluate the improvements from our implemented cloud and precipitation physics parameterization in the HWRF model.

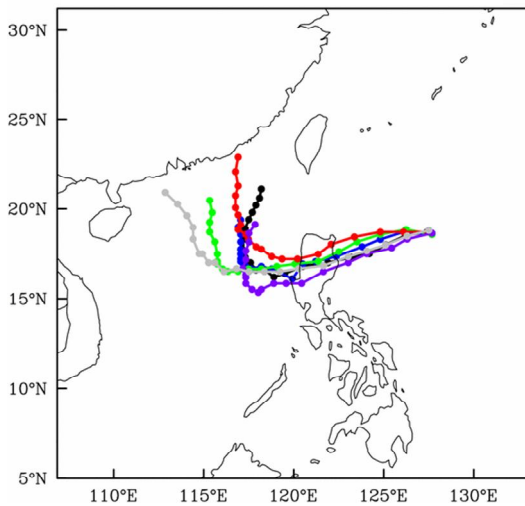
Initial time: 2010101500



Initial time: 2010101600



Initial time: 2010101700



- BST (JTWC)
- CTL (15km, BG)
- NOIN (15km, NOBG)
- GFS
- DI_KY
- DI_SM

Figure 25. WRF model forecast tracks at three different initial times and the JTWC best track. Different legends indicate results from different experiments: CTL is for 15 km uniform grids with bogus vortex (current real-time forecast at IPRC), NOIN the same as CTL but without use of the initial bogus vortex, GFS is GFS forecast, DI_KY means the new dynamical initialization scheme with KF cumulus parameterization scheme for outer model domains and YSU PBL scheme, DI_SM means the new dynamical initialization scheme with NSAS (new SAS scheme used in HWRF) cumulus parameterization scheme and the MYNN PBL scheme in the prediction experiments.

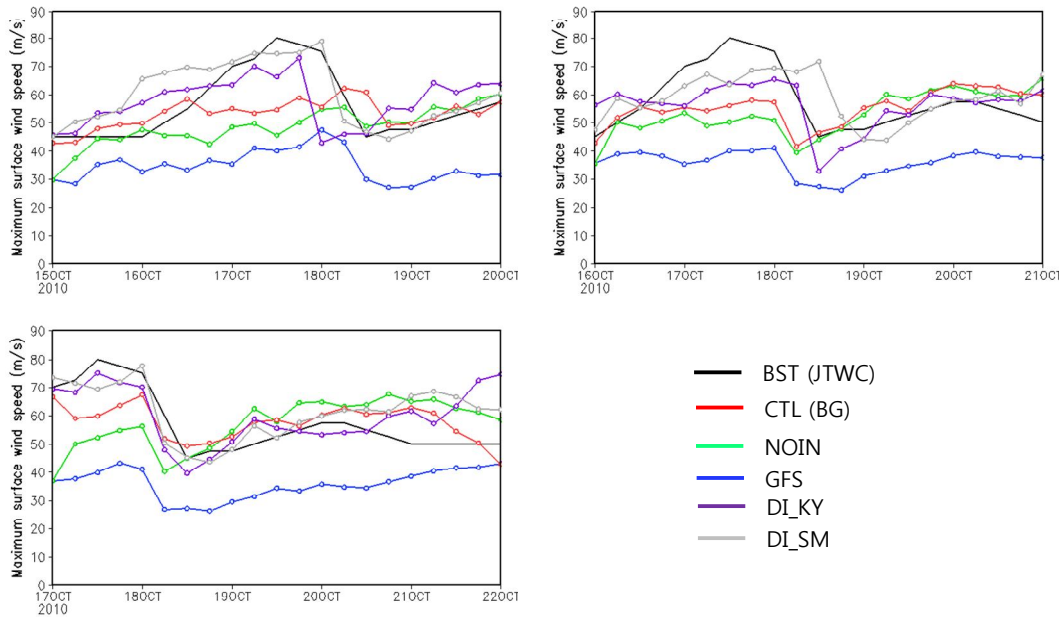


Figure 26. Evolution of storm intensity from JTWC best track and from different forecast experiments. See Figure 25 for the meanings of different legends.

In addition to Super Typhoon Megi, we also applied the new dynamical initialization scheme to other two storms (Figure 27) as a demonstration the effectiveness of the new scheme. We are evaluating the new scheme for more cases currently and will publish the results in a peer-review journal later this year. In particular, this allows us to test the new GFS cumulus parameterization used in the new version of the HWRf model.

i. Test of a new warm rain cloud microphysics including subgrid variability

The parameterization of warm rain processes is of crucial importance in determining cloud properties in any weather and climate models. Many current models treat the efficiency of autoconversion and accretion as free tuning parameters to adjust cloud properties so that simulated top-of-atmosphere radiative fluxes broadly agree with observations. This empirical tuning has various disadvantages. For example, the cloud lifetime indirect aerosol effect is very sensitive to details of the cloud parameterizations. In particular, taking into account the subgrid scale variability of cloud properties is the way to reduce the uncertainties and to avoid the empirical tuning. Recently a novel method to constrain autoconversion and accretion rates in atmospheric models has been constructed at the University of Hawaii in collaboration with scientists in the University of Wisconsin and France (Bennartz et al. 2011). The method offers two desirable features that might ultimately help to effectively eliminate autoconversion efficiency as a free tuning parameter in atmospheric models. Firstly, it can be constrained based on concurrent observations of column integrated cloud properties, namely cloud droplet number concentration, liquid water path, and precipitation rate. Secondly, the scale-dependency of autoconversion can be incorporated and resolved explicitly.

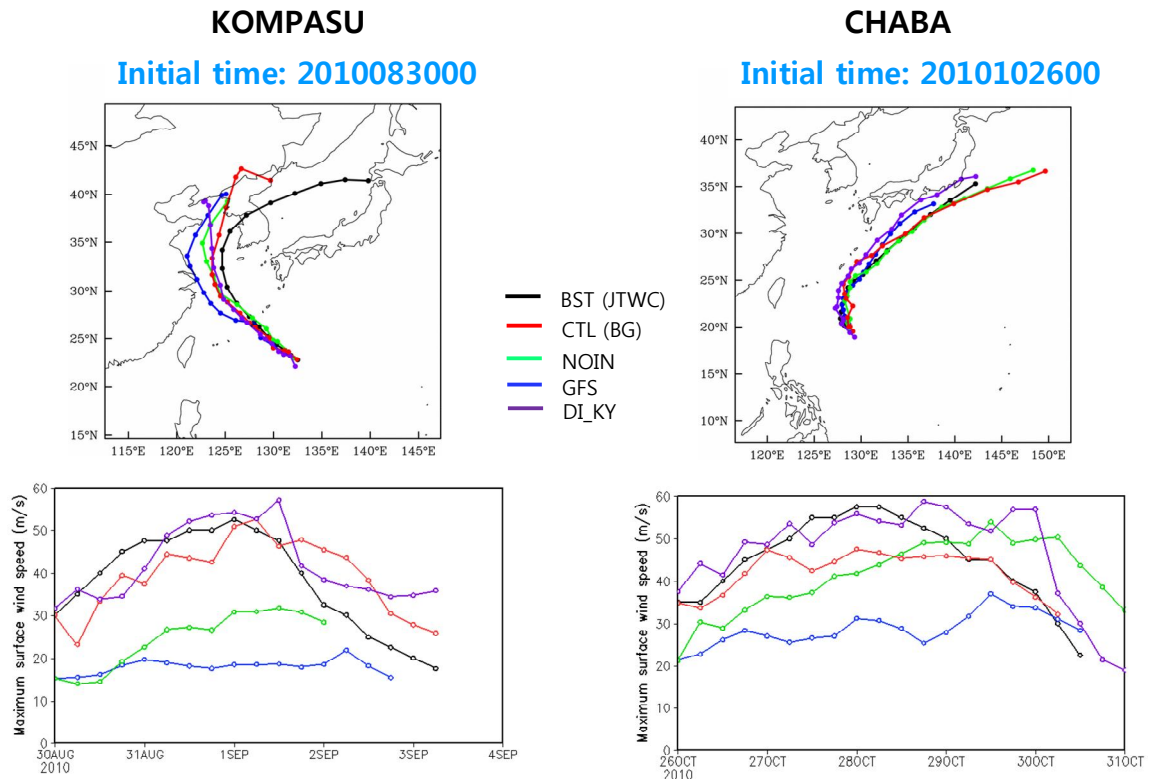


Figure 27. As in Figures 25 and 26 but for Typhoons Kompasu and Chaba (2010).

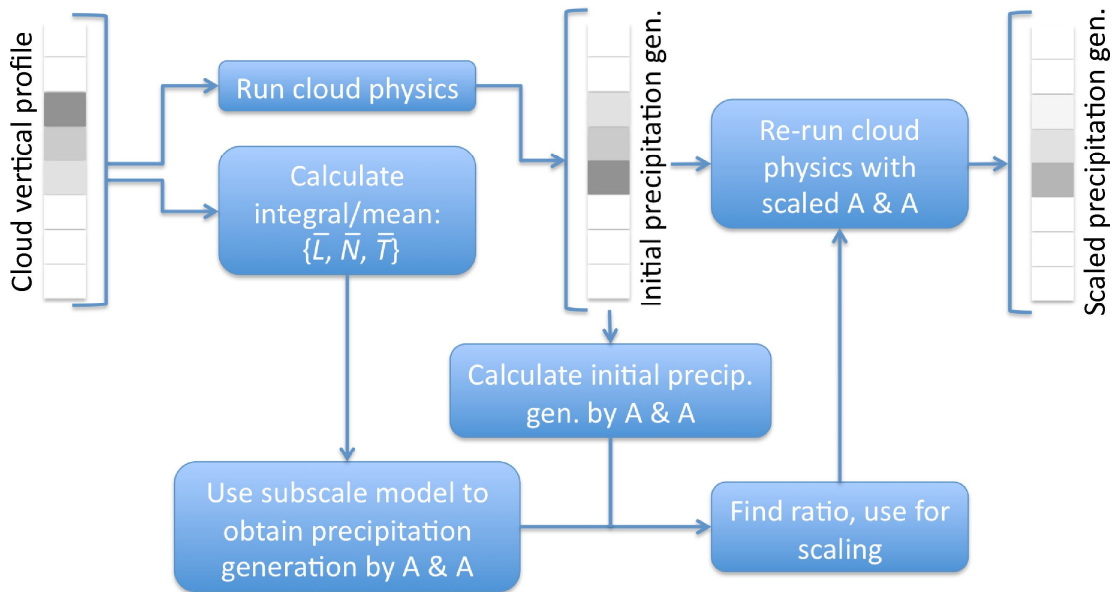


Figure 28. Schematic view of the implementation of the integral constraint method into the regional atmospheric model. The cloud microphysics scheme within the model is used to calculate the production of warm rain and its vertical distribution. The subscale model is used to linearly scale the cloud microphysics results to obtain the correct precipitation flux at cloud base. ("A & A": Autoconversion and Accretion) (Bennartz et al. 2011).

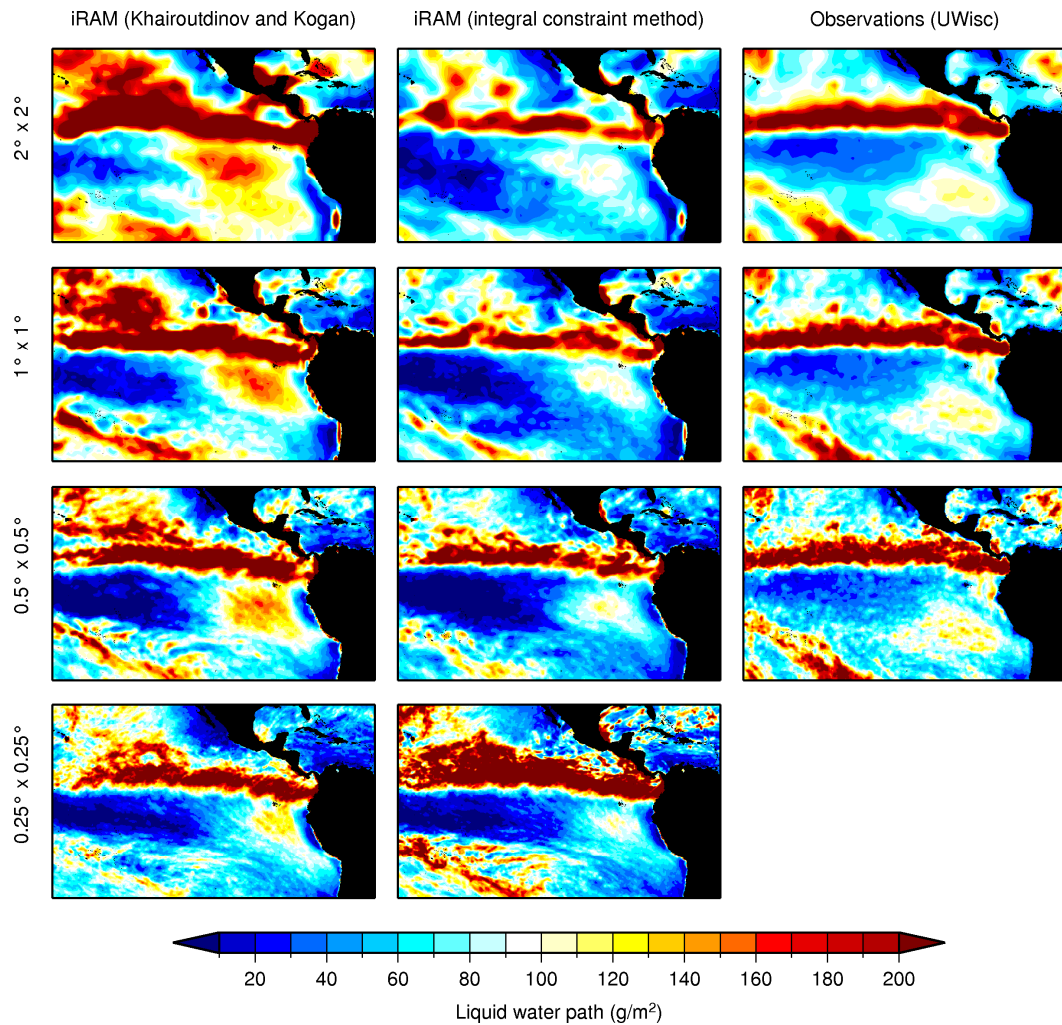


Figure 29. Monthly mean liquid water path from iRAM for October 2006 obtained with the original Khairoutdinov and Kogan [2000] autoconversion scheme (left column) and with the constrained autoconversion scheme (middle column) in comparison with satellite observations (right column). Shown are the horizontal resolutions (from top to bottom): $2^\circ \times 2^\circ$, $1^\circ \times 1^\circ$, $0.5^\circ \times 0.5^\circ$, and $0.25^\circ \times 0.25^\circ$. (Bennartz et al. 2011).

The new method was implemented into the University of Hawaii's atmospheric model iRAM developed by the PI. Figure 28 gives the flow chart to show how it wells in an atmospheric model. A series of test runs were performed at horizontal resolutions ranging from $0.25^\circ \times 0.25^\circ$ to $2^\circ \times 2^\circ$ for the eastern Pacific where warm rain cloud microphysics is dominated for the boundary layer clouds. The constrained approach was compared with a conventional approach commonly found in current weather and climate models. Comparisons with an observational climatology of cloud liquid water path reveal significant improvements, in particular a better consistency between different model resolutions (Figure 29). There are two limitations of this autoconversion scheme however: (1) it can only be applied to warm clouds and some assumptions will break down if there is a significant mixed or ice phase; (2) the scheme uses look-up tables, which are only available for certain horizontal resolutions. We can

extend the look-up table by implementing some kind of interpolation for horizontal resolutions that are not covered by the look-up table. While for the limitation (1) we may tune the scheme a little bit for application with mixed phase cloud microphysics for hurricanes.

This no-const extension reporting period (08/01/2011-01/31/2012)

j. Hindcasts for 2010 and 2011 western North Pacific TCs using the newly development dynamical initialization scheme using WRF

To evaluate the effectiveness of the newly developed dynamical initialization scheme introduced in section above, two sets of experiments are designed for TCs occurred over the Northwest Pacific in 2010 and 2011: the forecast run without the use of the dynamical initialization scheme (hereafter referred to as the CTL run) and the forecast run with the use of the dynamical initialization scheme (hereafter referred to as the DI run). The results from the two forecast runs are also compared with those from the GFS forecast (hereafter referred to as the GFS forecast). The initial condition in the CTL run is directly from the GFS analysis, while that in the DI run is the WRF output from the last cycle run as described in section 2b. Other model configurations in the two runs are identical.

In both forecast runs, the WRF contains a mother domain (DM1), an intermediate domain (DM2), and an innermost domain (DM3). The two-way moving nesting method is applied. Domain sizes (horizontal grid spacings) of DM1, DM2, and DM3 are 311×251 grid points (18 km), 271×271 grid points (6 km), and 211×211 grid points (2 km), respectively. The center of the mother domain is 5 (7) degrees to the north (northwest) from the observed TC center if the latitude of the observed TC center is north (south) of 20°N , while the centers of the two sub-domains are near the observed TC center. All domains have 28 vertical levels from the surface to the model top at 50 hPa. The time-steps for the model integration are 90 s, 30 s, and 10 s for DM1, DM2, and DM3, respectively. The forecast runs are initialized at 00 UTC or 12 UTC and integrated for 72 h.

The total number of TCs over the Northwest Pacific occurred in 2010 is 14, which is below the climatological mean. We selected 9 TCs with the duration longer than 4 days and conducted 38 forecasts for both the CTL and the DI runs. In addition, to demonstrate the robustness of the proposed new dynamical initialization we conducted 31 forecasts for 4 TCs occurred in 2011, which had intensity above typhoon (>64 knot) in their lifetime and showed different types of tracks. Therefore, in total 69 forecasts for 13 TCs in 2010 and 2011 were conducted in this study (Table 2). If the initial TC intensity in the GFS analysis at the initial forecast time is close to the observed, it is possible that the dynamical initialization results in the over-intensification of the TC. Therefore, the dynamical initialization scheme is skipped for the cases in which the maximum wind speed in the GFS analysis at the initial forecast time is within 90% of the JTWC best-track data. There are about 4 cases (about 5%) of our total forecasts that the dynamical initialization is skipped. For these cases, the results from the CTL run are used in the verification. To verify the TC forecasts, the JTWC best-track data are used for TCs in 2010, and the JTWC warning information is used for TCs in 2011 since the JTWC best-track data for TCs in 2011 is not available by the time we performed the verification.

The position error and intensity error of the CTL and DI runs are calculated from the results of DM2, since the instantaneous result of DM2 with a time step of 30 s implies a time mean of 30 s to one minute, comparable to the best-track intensity in terms of maximum surface

wind speed, which is assumed to be a 1-minute mean. Figure 30 shows the homogeneous position and intensity errors averaged for the 69 forecasts. The position errors tend to increase as the forecast time increases in all runs. At all lead times, the GFS forecasts show the largest position errors, and the DI run has smaller position errors than the CTL run. The initial position error of the DI run is much smaller than that of the GFS analysis and of the CTL run due to the use of the relocation method. However, the DI run still has slight initial position error because of the skipping of the relocation method in the forecasts when the TC core is affected by the topography. Also, merging the relocated axisymmetric vortex component with the environmental component after the relocation can cause slight position difference in the DI run due to the asymmetric nature of the environmental pressure field. The improvements from the dynamical initialization are more obvious in intensity forecasts. The GFS forecast shows the largest intensity errors. The CTL run reduces the intensity error to about 10 m s^{-1} at all lead times except for the initial time. The DI run further reduces the intensity errors due to the dynamical initialization, in particular, in the first 24 h forecasts. Therefore, the improvement due to the use of the dynamical initialization scheme decreases as the forecast time increases.

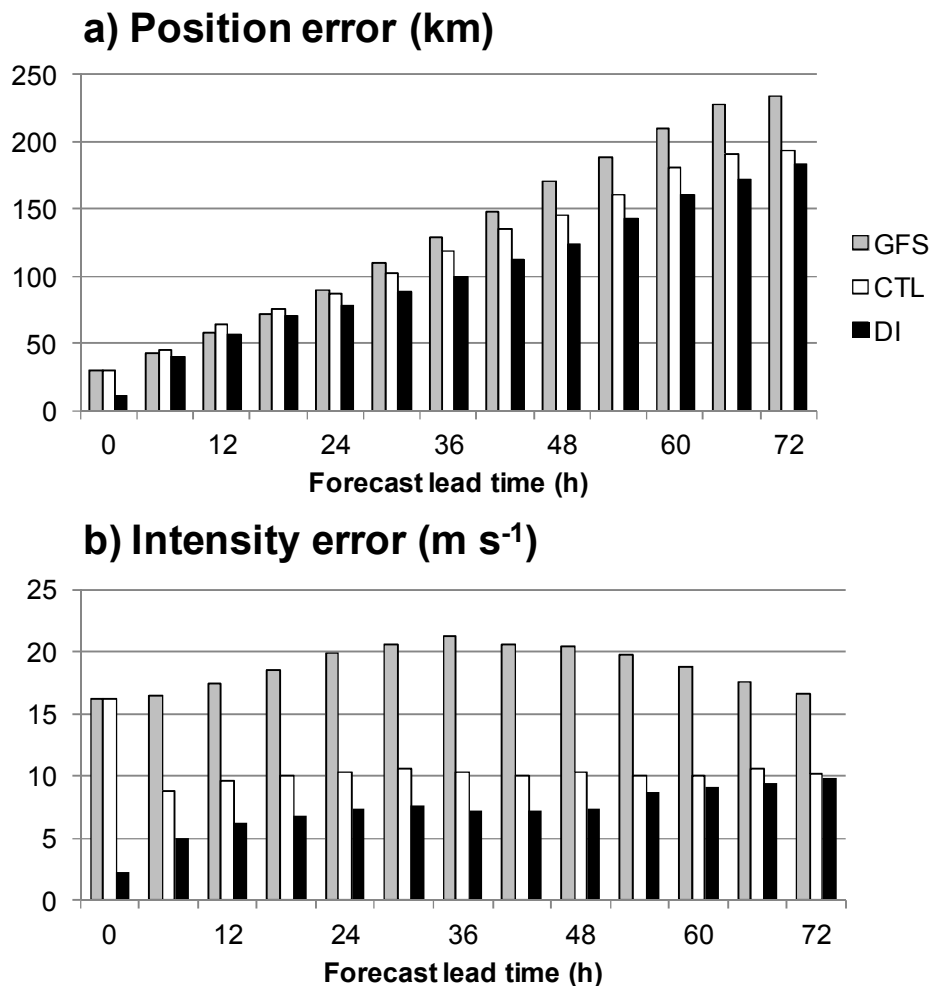
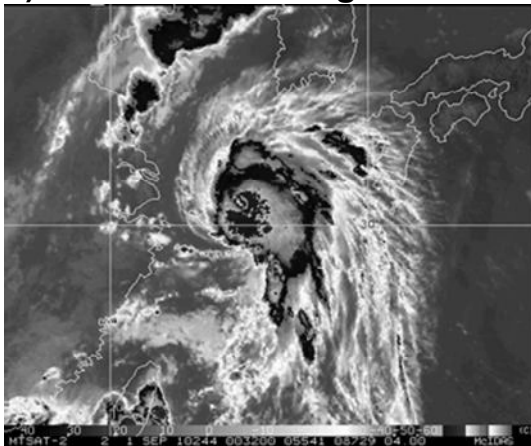


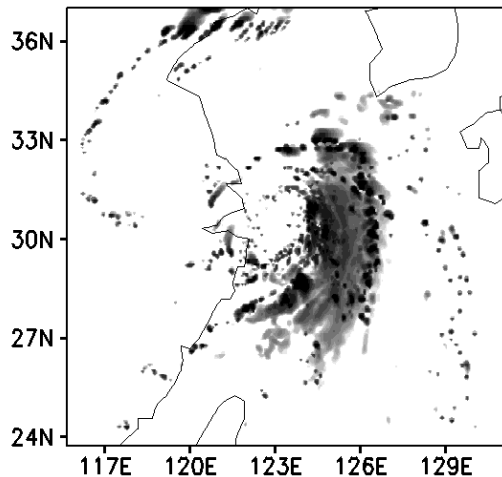
Figure 30. Homogeneous position (km) and intensity (m s^{-1}) errors of the GFS forecast, and the CTL and DI runs averaged for 69 forecasts

Compared with the GFS forecast, the CTL run decreases the 72-h mean position and intensity errors by about 10% and 45%, respectively. This means that the mesoscale WRF model with high model resolution can improve the TC forecast in terms of track and intensity even if no any TC initialization scheme is employed. Compared with the CTL run, the position and intensity errors in the DI run are further reduced by about 15% and 30%, respectively. Therefore, the dynamical initialization improves both the track and intensity forecasts. The improved TC structure due to the use of the dynamical initialization scheme can be seen from a case for Typhoon Kompasu (2010) as shown in Fig. 31. In the CTL run, the inner core structure is quite asymmetric and only the major outer spiral rainband is captured. In contrast, the DI run produces the horizontal distribution of cloud and precipitation in Typhoon Kompasu. The simulated inner-core structure and two outer spiral rainbands are in good agreement with the satellite observation.

a) Enhanced IR Image



b) CTL



c) DI

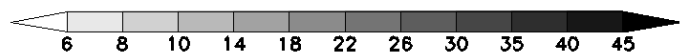
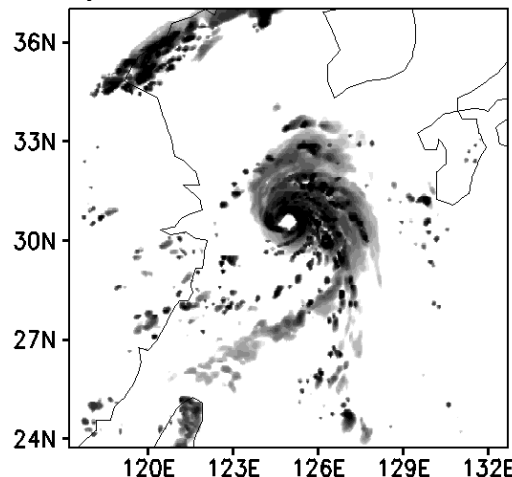


Figure 12. (a) Enhanced IR image of MTSAT satellite and (b, c) the horizontal distributions of the simulated radar reflectivities (dBZ) at the peak intensity of the observed Typhoon Kompasu (00 UTC 1 September 2010 after 24 h of integration). Forecast initial time is 00 UTC 31 August 2010.

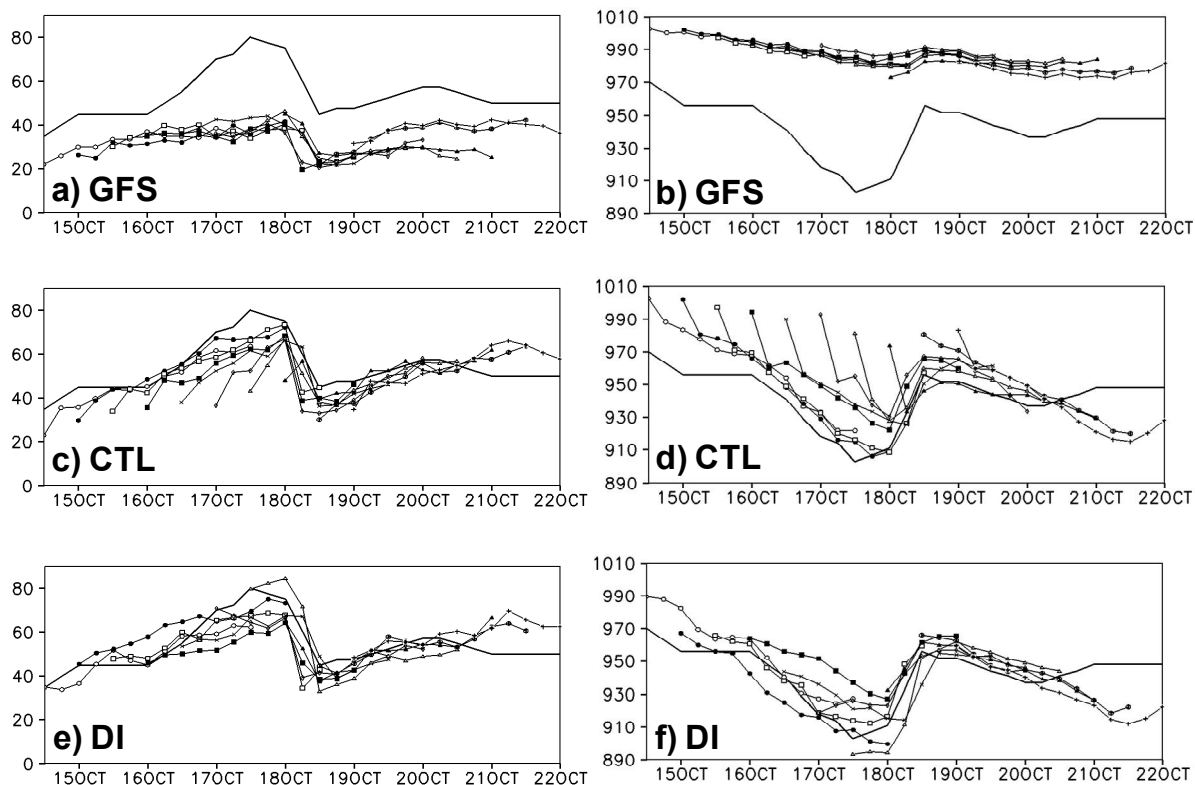


Figure 32. Temporal evolution of the maximum surface wind ($m s^{-1}$, left panels) and the central sea level pressure (hPa, right panels) for Typhoon Megi from the JTWC best-track data (solid), the GFS forecast, and the CTL and DI runs. Different marks are used to distinguish forecasts with 10 different initial times from 12 UTC 14 October 2010 to 00 UTC 19 October 2010.

Typhoon Megi was the strongest typhoon over the Northwest Pacific in 2010 resulting in huge damages in the Philippines, Taiwan, and Mainland China. It formed southeast of Guam and moved westward to the Philippines. After passing over the Philippines, it turned to the north and moved toward South China. The tracks predicted from three forecasts are similar to each other and close to the best track (Fig. 14). All forecasts capture the landfall over the Philippines and the northward turning after the landfall. The 72 h mean position errors averaged for 10 forecasts are less than 100 km in all runs. Nevertheless, the DI run has position error about 30% smaller than the GFS forecast.

The temporal evolutions of the maximum surface wind and central sea level pressure predicted by the three forecasts for Typhoon Megi are shown in Fig. 32. It is not surprising that the GFS forecast underestimates the intensity of Typhoon Megi. The CTL run considerably improves the evolution of the typhoon intensity, but there are significant initial shocks in the first 6 h forecast. The initial shocks in the CTL run are related to the discrepancies in dynamical balance in the interpolated high-resolution to the WRF model from the low-resolution GFS analysis and also the spin-up of physics of the forecast model. It seems that it takes about 12 h for a balance adjustment and the spin-up of the model physics in the CTL run. In contrast, the initial shocks do not appear in the DI run because the physical and dynamical inconsistencies and any possible imbalances are damped during the cycle runs in the dynamical initialization. The

warm startup of model physics also contributes to a smooth evolution of the storm intensity in the DI run. (The manuscript has been submitted to Monthly Weather Review)

k. Configuration of the newly released HWRF model for the North Atlantic

We have configured the EMC HRF model for the North Atlantic. The model is two-way nested with the outer domain consisting of 216*432 grid points with a resolution of 0.18 degrees and the inner nested domain of grid points 61*100 with a resolution of 0.06 degrees. The model has 42 sigma levels with the model top at 50hPa. The model physics are the cloud microphysics of the Ferrier Scheme, the Simplified Arakawa-Schubert (SAS) scheme, the surface layer scheme nearly identical to the GFDL's scheme with the momentum roughness and the enthalpy roughness calculated based on Kwon et al. (2010) and Black et al. (2007), the slab land surface model of the GFDL, the non-local PBL scheme as the GFDL operational hurricane model, and the GFDL longwave and shortwave schemes. These are not an optimal combination of different physics parameterizations, while just have the model run smoothly on our local PC cluster. We have performed two forecast experiments for Hurricane Irene (2011). The model predicts the track quite well but too weak intensity (Figs. 33 and 34). We can see that even for the initial time 00 UTC August 24, the intensity is very close to the observed, the predicted intensity is still much weaker than the observation. This indicates that the model physics of the HWRF needs to be improved. We will use the remaining time to work toward improved cloud and precipitation physics with this model configuration.

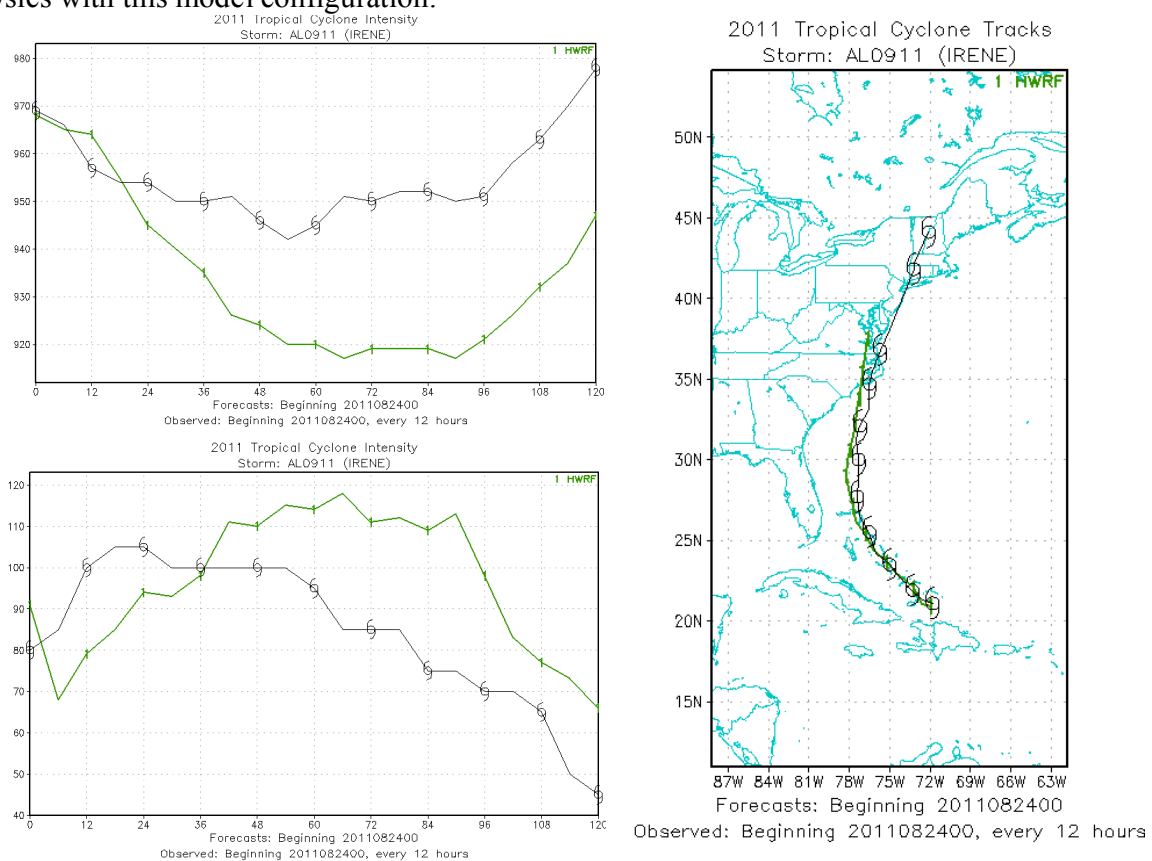


Figure 33. The HWRF model predicted Hurricane Irene's intensity (left) and track (right) with initial time at 00 UTC August 24, 2011.

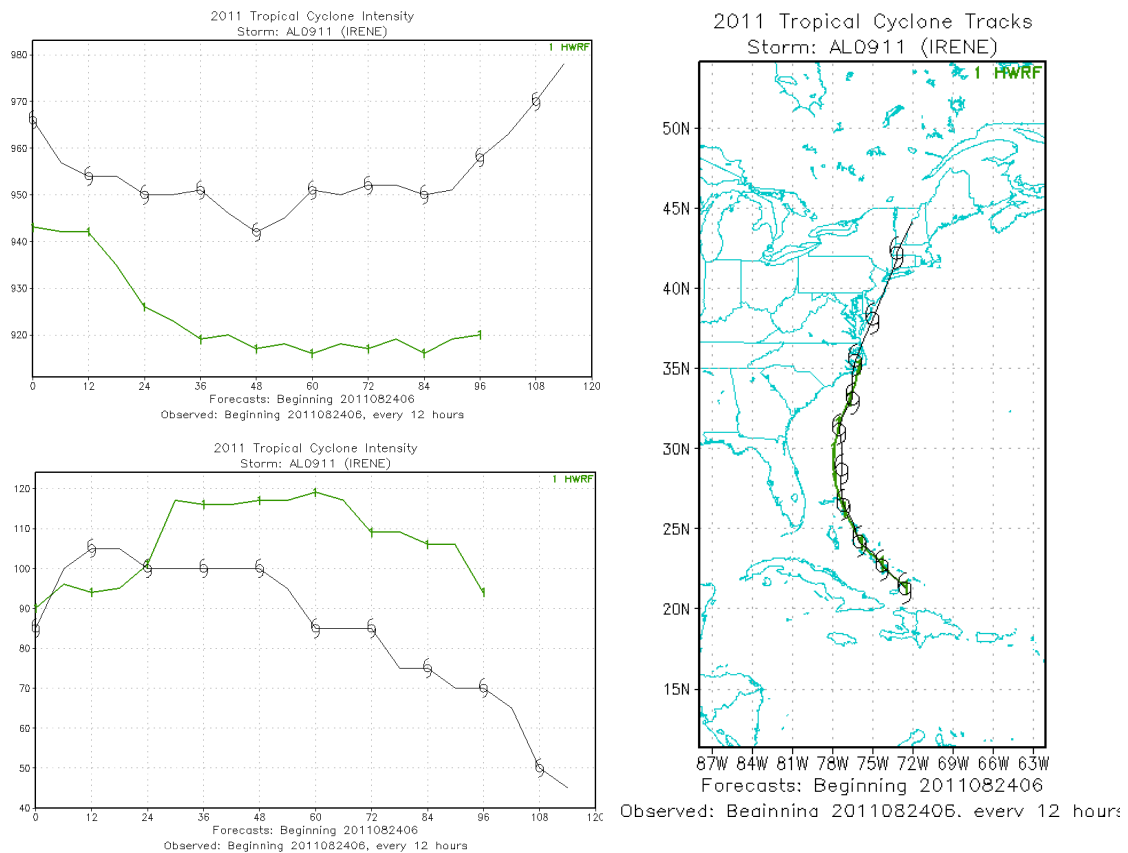


Figure 34. The HWRf model predicted Hurricane Irene’s intensity (left) and track (right) with initial time at 06 UTC August 24, 2011.

WORK PLAN

We will use the remaining 5 months to work on improving new operational settings of the HWRf model and continue our effort toward improved prediction of hurricane structure and intensity changes. We will also document the improvements in journal publications and research reports by the end of this project.

References

- Bennartz, R., A. Lauer, and J.-L. Brenguier, 2011: Scale-aware integral constraints on autoconversion and accretion in regional and global climate models. *Geophys. Res. Lett.*, **38**, L10809. IPRC-781.
- Cha, D.-H., and Y. Wang, 2012: A dynamical initialization scheme for real-time forecasts of tropical cyclones using the WRF model. *Mon. Wea. Rev.*, (submitted).
- Khairoutdinov, M., and Y. Kogan (2000), A new cloud physics parameterization in a large-eddy simulation model of marine stratocumulus, *Mon. Wea. Rev.*, *128*(1), 229-243.
- Korolev, A. V., and I. P. Mazin, 2003: Supersaturation of Water Vapor in Clouds. *J. Atmos. Sci.*, **60**:24, 2957-2974
- Korolev, A. V., 2007: Limitations of the Wegener–Bergeron–Findeisen mechanism in the evolution of mixed-phase clouds. *J. Atmos. Sci.*, **64**, 3372-3376

- Phillips, V. T. J., and L. J. Donner, 2006: Cloud microphysics, radiation and vertical velocities in two- and three-dimensional simulations of deep convection. *Q. J. R. Meteorol. Soc.*, **132**, 3011-3033
- Phillips, V. T. J., Donner, L. J., and S. Garner, 2007: Nucleation processes in deep convection simulated by a cloud-system resolving model with double-moment bulk microphysics. *J. Atmos. Sci.*, **64**, 738-761
- Phillips, V. T. J., Andronache, C., Christner, B., Morris, C. E., Sands, D. C., Bansemer, A., Lauer, A., McNaughton, C., and C. Seman, 2009: Potential impacts from biological aerosols on ensembles of continental clouds simulated numerically. *Biogeosciences*, **6**, 1-28
- Wang, Y., 2007: A multiply nested, movable mesh, fully compressible, nonhydrostatic tropical cyclone model - TCM4: Model description and development of asymmetries without explicit asymmetric forcing. *Meteor. Atmos. Phys.*, **97**, 93-116.
- Wang, Y., 2009: How do outer spiral rainbands affect tropical cyclone structure and intensity? *J. Atmos. Sci.*, **66**, 1250-1273.
- Wang, Y., S.-P. Xie, H. Xu, and B. Wang, 2004: Regional model simulations of marine boundary layer clouds over the Southeast Pacific off South America. Part I: Control experiment, *Mon. Wea. Rev.*, **132**, 274-296.
- Xu, J., and Y. Wang, 2010: Sensitivity of the simulated tropical cyclone inner-core size to the initial vortex size. *Mon. Wea. Rev.*, **138**, 4135-4157.